energies

MDPI

Review

Molecular Simulation Techniques as Applied to Silica and Carbon-Based Adsorbents for Carbon Capture

Basil Wadi [1,2,*], Ayub Golmakani [2], Tohid N.Borhani [3], Vasilije Manovic [2] and Seyed Ali Nabavi [2,*]

[1] Chemical Engineering Department, University of Ottawa, Ottawa, ON K1N 6N5, Canada
[2] Centre for Climate and Environmental Protection, Cranfield University, Bedford MK43 0AL, UK
[3] Faculty of Science and Engineering, University of Wolverhampton, Wolverhampton WV1 1LY, UK
* Correspondence: bwadi068@uottawa.ca (B.W.); s.nabavi@cranfield.ac.uk (S.A.N.)

Abstract: There has been ongoing interest in research to mitigate climate change through carbon capture (CC) by adsorption. This guideline is meant to introduce computational chemistry techniques in CC by applying them to mesoporous structures and disordered morphologies. The molecular simulation techniques presented here use examples of literature studies on silica and carbon-based adsorbents. An initial summary of molecular simulation techniques and concepts is first presented. This is followed by a section on molecular simulation applications in mesoporous amorphous silica, both functionalized and not. Novel strategies to validate and output useful results are discussed, specifically when modelling chemisorption. The use of computational chemistry to build upon experimental results is reviewed, and a similar summation is presented for carbon-based adsorbents. The final section provides a short review of computational chemistry methods in novel applications and highlights potential complications. Computational chemistry techniques provide a streamlined method of gathering data across a range of conditions. Alongside experimental studies, these techniques can provide valuable information on underlying molecular mechanisms. This paper aims to be a starting point for navigating these numerical methods by providing an initial understanding of how these techniques can be applied to carbon capture while clarifying the current and inherent limitations present.

Keywords: low-carbon technologies; carbon capture; molecular simulation

check for updates

Citation: Wadi, B.; Golmakani, A.; N.Borhani, T.; Manovic, V.; Nabavi, S.A. Molecular Simulation Techniques as Applied to Silica and Carbon-Based Adsorbents for Carbon Capture. *Energies* **2023**, *16*, 5013. https://doi.org/10.3390/en16135013

Academic Editor: María Pilar Lisbona

Received: 8 March 2023
Revised: 23 May 2023
Accepted: 29 May 2023
Published: 28 June 2023

Copyright: © 2023 by the authors. Licensee MDPI, Basel, Switzerland. This article is an open access article distributed under the terms and conditions of the Creative Commons Attribution (CC BY) license (https://creativecommons.org/licenses/by/4.0/).

1. Introduction

The National Centers for Environmental Information (NCEI) published an assessment of the Global Climate in 2020, reporting the average surface temperatures in 2019 as the second highest since 1880, with an estimated anthropogenic warming between 0.1 and 0.3 °C per decade [1,2]. As this trend foresees damage to ecosystems worldwide, there has therefore been an increasing interest in developing carbon capture and storage technologies. Such initiatives are motivated by the Climate Change Act released by the UK government, to achieve the vision of a carbon neutral society in the long term [3].

Targeting the decarbonization of already established industrial plants is a harmonic and feasible method in achieving emission goals while balancing economic implications of the transition to a net-zero emissions society. Carbon capture as applied to post-combustion is one method, and addresses the already operating fossil fuel plants, considered to account for 81% of energy generation worldwide, as reported in 2017 by the International Energy Agency (IEA) [4]. Alternatively, pre-combustion capture targets the removal of CO_2 prior to usage, and is employed in biogas reforming, coal gasification or steam reforming of natural gas. Additionally, biogas upgrading can be used to purify biogas and place it as a source of energy of net-zero to negative carbon emission. Regardless of the method of capture, there has been an increasing level of research towards the incorporation of carbon capture and biogas upgrading technologies into the current energy industry. Such studies can be

conducted through experimental or computational methods. However, in recent years, the rise of higher computational power has opened opportunities for the further incorporation of simulation software in solving complex theoretical equations. These tools have provided insight into interaction mechanisms both at a micro and macro scale, often complementing traditional experimental techniques. In terms of studying the adsorption and diffusion of gas molecules on solids, Density Functional Theory (DFT), Monte Carlo (MC) and molecular dynamics (MD) software are powerful tools and, when correctly employed, can accurately re-create experimental data. Additionally, they provide information on material properties and molecular interactions costly or difficult to measure within a laboratory.

A multitude of reviews outlining the experimental, and technological milestones and breakthroughs in carbon capture and biogas upgrading can be found. Table 1 summarizes some reviews on simulation within a broader context of Gas Adsorption. For adsorption through physical interactions, Zeolites are frequently studied as they have been shown to have a high capacity for CO_2 adsorption at low production costs. Furthermore, their potential for enhancement through metal cation modification makes them more promising, although regeneration costs can be energy intensive [5]. Abdulrasoul et al. [6] thoroughly reviewed the influence of compositional properties on a system's molecular interactions by Monte Carlo and Molecular Dynamics. Metal Organic Frameworks (MOFs) are also widely studied in a range of applications as a result of their inherent structural adjustability during synthesis [7]. A recent review concentrating on general applications of MOFs by Sturluson et al. [8] looked at the role molecular simulation (MS) can play in screening thousands of experimentally synthesized MOF structures. This is necessary to streamline the choice of adsorbent composition, and direct laboratory work towards achieving a desired adsorption property. From a different perspective, Getman et al. [9] prepared a comprehensive review on molecular modelling of Hydrogen, Methane, and acetylene storage in MOF and Covalent Organic Framework (COF) materials, providing detailed insight on applications, simulation techniques, and software limitations relevant to more than just gas storage.

The mentioned reviews cover a cornucopia of literature related to the application of computational methods in adsorbent discovery and study. However, there are few that concentrate on the design methodologies for mesoporous and morphologically asymmetric adsorbents, while also aiming to present an introductory guideline for non-chemists to better understand what computational chemistry techniques may entail. The enhanced selectivity towards CO_2 by amine functionalization and the urgency towards more efficient carbon capture has extended the study of adsorbent development towards many novel materials beyond zeolites and MOFs. There is also a growing interest in the development of carbon capture technology amongst a diverse range of disciplines.

Herein, the feasibility of utilizing molecular simulation techniques to better understand mesoporous and heterogenous adsorbents, as applied to amorphous silica, carbon-based materials is presented, while simultaneously aiming to be an introductory doorway towards utilizing such techniques for a multidisciplinary audience.

Section 1 will provide an overview of computational chemistry, and the methods associated with them that are primarily used in carbon capture adsorption systems. The subsequent sections are divided on a material specific basis, starting with mesoporous silica, followed by its functionalized form, and similarly with carbon-based adsorbent, followed by any functionalization studies. A final section which introduces disordered polymeric structures is also included to discuss potential novel applications of molecular simulation techniques.

Table 1. Reviews on applications of computational simulation in carbon capture.

Reference	Scope of Review
Abdelrasoul et al. [6]	Discusses the benefits of computational studies through Monte Carlo and Molecular Dynamics in better understanding adsorbent properties in diffusion and adsorption processes. This includes detailed revision of cation–zeolite–adsorbate interactions and their influence on structural dynamics and adsorbent properties.
Sturluson et al. [8]	Gas adsorption simulations and their use in the discovery of high-performing MOF structures. A comprehensive list of applications is reviewed from methane, hydrogen, and oxygen storage to CO_2 capture, and xylene enrichment.
Wang et al. [10]	Molecular Simulation Methods through DFT, GCMC, and MD applications in shale matrix. This is specific to understanding gas transport in shale matrix through studying the intermolecular interactions that play a part in the amount of adsorbed gas on shale matrix and dissolved gas in the bulk [10].
Ruiperez [11]	The use of quantum chemistry in characterising polymer material through reaction modelling for polymerisation, dynamic bonds and associated interactions, and analysis of intermediate and excited states.
Mansour et al. [12]	Experimental and numerical modelling for carbon capture through physisorption. Simulation via mathematical modelling at a macro scale rather than molecular scale is reviewed in fixed bed columns utilizing MOFs, zeolites, and carbon-based materials.
Li et al. [13]	Methods of macro modelling of CO_2 and N_2 adsorption, and a screening methodology for the representative equation group of each specific system. The equation group includes parameters representing the kinetics, equilibrium, momentum loss and heat loss within a system.
Getman et al. [9]	Adsorption modelling of Methane, Hydrogen, and Acetylene storage in MOFs and COFs through GCMC and Quantum calculations. In-depth discussions on simulation techniques for parameterization and system dependency. An analysis of functionalization and Cation-doped adsorbents is included, including limitations in modelling such systems.
Rafiee and Moghadam [14]	Techniques in modelling the structures of carbon nanotube, and their effectiveness in predicting the mechanical behaviour of CNTs. A detailed analysis of computational time, applicability to larger systems, as well as accuracy in representations as a continuum structure compared to atomistic modelling.

The type of adsorbate–adsorbent interaction to be studied dictates the appropriate simulation method for each system. As a result, a combined set of techniques are necessary to gain a full picture of adsorption mechanism in gas applications, specifically when chemisorption is considered. In this paper, various methods used in preparing the adsorbent structure, the process conditions considered, and the choice of forcefield for each are described followed by the insights gained, the limitations faced, and the workarounds employed to overcome them.

This synopsis aims to provide engineers with a framework for using MS methodology in gas adsorption applications. The benefits of MS span from understanding the molecular level mechanisms of adsorption processes to generating large, simulated data sets for further screening. This paper highlights techniques of MC and DFT modelling with only silica and carbon-based adsorbents with the hopes that the presented methods may be transferred towards alternative applications.

2. Simulation Methods

Molecular simulation relies on statistical thermodynamics to define each molecule's position and state of existence [15]. In Monte Carlo and Molecular Dynamic simulations, a subset of molecular mechanics (MM), the translation of molecules is based on concepts of Brownian motion, defined as the random motion of particles at a microscopic level [16]. The average of this movement at equilibrium can provide realistic information on the macroscopic properties of a sample. Compared to quantum chemical methods, MM simulations provide less accuracy in predicting structures and exact energies but are significantly less computationally demanding and therefore convenient approximations [17]. In MM modelling, the molecular energy is defined by both inter- and intramolecular forces that are dictated by user-assigned force field parameters. The following section discusses the fundamentals of these force fields and major factors to consider for their use.

2.1. Molecular Mechanics Methods

The rise of higher computational power has opened opportunities for the better use of simulation software in providing insights to adsorption mechanisms both at a molecular and macro scale. At the molecular scale, Molecular Mechanics is often used to simulate fluid movement within specified boundary conditions. Molecular dynamic (MD) is a subset of Molecular Mechanic (MM) simulations and relies on Newton's law of motion to simulate the movement of particles within a system [18]. This follows an integration of Newton's equation of motion across a specified time step:

$$\overrightarrow{F_i} = m_i \frac{d^2 \overrightarrow{r_i}}{dt^2} \quad (1)$$

where F is the force, m_i is mass, r_i is the position of the particle, and t is time.

The movement of particles follows user-specified inputs and can include the insertion/deletion of particles; however, this specific removal can affect the continuity of Newton's equation, and limits MD simulations in being applied for gas adsorption studies since the Grand Canonical Ensemble (GCMC) cannot be utilized [15]. MD is thus used for diffusion and heat transfer behaviour through transport phenomenon analysis; by maintaining the total of the energy of the system constant the above equation is solved through the micro-canonical ensemble expressed as NVE [15].

When applying MD in gas adsorption, there are only hybrid methods to simulate the changing energy within the system, while maintaining a constant chemical potential or fugacity. This makes MD simulations not as straightforward in reproducing experimental gas adsorption behaviour compared to GCMC. Nonetheless, it can aid in deriving important system information, such as determining energy contributions to binding, interactions of contaminants with the surface, or identifying favourable adsorption sites [19]. Software used for these simulations includes open-source LAMMPS, GROMACS, and OpenMM. LAMMPS can be considered quite comprehensive having larger forcefield databases with capabilities of Monte Carlo (MC) and MD, while GROMACS offers enhanced post-processing tools. Both offer faster computer processing compared to OpenMM [20]. Although there have been studies of MD in CCS, particularly for sequestration, gas adsorption is often simulated using MC and this method of calculation is discussed in the next section.

In the next section, Monte Carlo calculations will be discussed. MC is a powerful sampling method used in molecular simulation software to re-create experimental adsorption data through the employment of the GCMC ensemble and producing essential thermodynamic information over a wide range of process conditions.

2.1.1. Forcefields in Molecular Mechanics

In replicating intramolecular interactions of a system, an expanded forcefield equation that accounts for all atomic contributions within a certain system is used [15,21]. This equation describes internal molecular energy contributions and is parametrized through a

rigorous procedure that fits thermodynamic data to forcefield parameters and can include bond length, bond angle, bond torsions, and any further contributions deemed influential to replicate experimental properties. The accuracy of the system is affected by the decision of which key elements are included within the force field (FF) equation; there are many forms of the FF equation utilizing either generic or specific parameter fitting and Equation (2) is one representative example of energy contributions within a forcefield [21,22]. The first three terms represent internal or intramolecular energy contributions while the last term applies to external or non-bonded influences. It is important to note that electron properties are not taken into account, and therefore reactions and interactions involving the exchange of electrons are not modelled [23].

$$U = E_{Bond} + E_{Angle} + E_{Torsion} + E_{NonBonded} \tag{2}$$

$$E_{Bond} = \frac{1}{2}k(r - r_0)^2 \tag{3}$$

$$E_{Angle} = \frac{1}{2}k_\alpha(\theta - \theta_0)^2 \tag{4}$$

$$E_{Torsion} = \frac{1}{2}k(1 - COS(2\chi)) \tag{5}$$

$$E_{NonBonded} = E_{VdW} + E_{Coulomb} \tag{6}$$

where r_0 is the reference bond length, k is the force constant, is the reference bond angle, k_α is the α force constant, and χ is the out-of-plane angle.

In modelling the intermolecular forces from the dispersion and repulsive energy of a non-bonded (E_{VdW}) interacting set of atoms within a system, the Lennard-Jones (LJ) potential is often used to represent the van der Waals contributions. The LJ potential equation has two forms designated as the 12-6 and 9-6 potential and the form used depends on the forcefield chosen and modelling method. Emami et al. [24] prepared a database for modelling silica surfaces and demonstrated the inability of generalizing LJ parameters for varying force fields, in order to accurately model real systems, they assigned different LJ potential values based on the energy equation or force field being used [24]. In the LJ equation, the repulsive force is represented by $(\sigma_{ij}/r_{ij})^{12}$ and the attractive forces by $(\sigma_{ij}/r_{ij})^6$. The adjustment of the power variable in the 9-6 form of the equation decreases the contribution of repulsive forces to the energy calculation; however, the 12-6 is more often found in Monte Carlo software and used for gas adsorption studies, and is expressed with the following equation:

$$E_{VdW} = \sum_{\substack{i,j \\ i<j}} 4\varepsilon_{ij}\left(\left(\frac{\sigma_{ij}}{r_{ij}}\right)^{12} - \left(\frac{\sigma_{ij}}{r_{ij}}\right)^{6}\right) \tag{7}$$

where σ in Angstrom is the distance at which intermolecular potential is zero, ε is the depth of potential well or how strong two particles attract each other, and r is the interatomic distance in Angstrom.

To reconstruct the interaction parameters σ, ε, and r for two atoms, a combination rule must be chosen. The Lorentz–Berthelot (LB) mixing rule is widely used in CO_2 gas adsorption studies, but has been shown to be outperformed by the Kong rule in certain systems, such as n-alkane-CO_2 mixtures [25]. A simple calculation testing each combination rule can demonstrate their effect on results, Delhommelle and Millie [26] demonstrated the variation between LB, Kong, and Waldman–Hagler (WH) combination rules in predicting equilibrium properties of Neon, Argon, and Krypton gases. They showed that the Kong

combination rule predicted the closest results of liquid properties and co-existence curves for the listed gases.

LB rule:

$$\sigma_{ab}^{LB} = \frac{\sigma_{aa} + \sigma_{bb}}{2} \tag{8a}$$

$$\varepsilon_{ab}^{LB} = \sqrt{\varepsilon_{aa}\varepsilon_{bb}} \tag{8b}$$

Kong rule:

$$\sigma_{ab}^{K} = \left\{ \frac{\left[\left(\varepsilon_{aa}\sigma_{aa}^{12}\right)^{\frac{1}{13}} + \left(\varepsilon_{bb}\sigma_{bb}^{12}\right)^{\frac{1}{13}} \right]^{13}}{2^{13}\sqrt{\varepsilon_{aa}\sigma_{aa}^{6}\varepsilon_{bb}\sigma_{bb}^{6}}} \right\}^{\frac{1}{6}} \tag{9a}$$

$$\varepsilon_{ab}^{K} = \frac{2^{13}\varepsilon_{aa}\sigma_{aa}^{6}\varepsilon_{bb}\sigma_{bb}^{6}}{\left[\left(\varepsilon_{aa}\sigma_{aa}^{12}\right)^{\frac{1}{13}} + \left(\varepsilon_{bb}\sigma_{bb}^{12}\right)^{\frac{1}{13}} \right]^{13}} \tag{9b}$$

WH rule:

$$\sigma_{ab}^{WH} = \left[\frac{\sigma_{aa}^{6} + \sigma_{bb}^{6}}{2} \right]^{\frac{1}{6}} \tag{10a}$$

$$\varepsilon_{ab}^{LB} = \frac{2\sigma_{aa}^{3}\sigma_{bb}^{3}}{\sigma_{aa}^{6} + \sigma_{bb}^{6}} \sqrt{\varepsilon_{aa}\varepsilon_{bb}} \tag{10b}$$

In the approximation of electrostatic and quadrupole contributions, atomic partial charges are used to represent them directly through Coulombs law.

$$E_{Coulomb} = \sum_{\substack{i,j \\ i<j}} \frac{1}{4\pi\varepsilon_o} \frac{q_i q_j}{r_{ij}} \tag{11}$$

In Equation (11), q_i, and q_j represent the partial charges of the interacting atom pair, r_{ij} is the separation distance, ε_o is the vacuum permittivity defined as permittivity of free space and is a constant equal to 8.85419 $\times$ 10^{-12} C^2/N-m^2. Considering that many simulation techniques account for intermolecular forces by only including parameters of partial charge and LJ potentials, polarization energy is thus accounted for in MC and MD simulations through the specific values assigned to these variables [9].

2.1.2. Generic Forcefields in Molecular Mechanics

The dependency of simulation results on the parameters chosen has led to focused study into the approximation of forcefield parameters, and many all-purpose forcefields have emerged, with some carefully fitted to specific systems such as the MM2, Dreiding, UFF, AMBER, OPLS, and TraPPE [27].

The Dreiding [28] and UFF [29] forcefields are examples of generic forcefields parameterized for a broad set of molecules and systems. They have been shown to successfully predict structural geometries of crystals as well as adsorption capacity and selectivity in a variety of adsorbent types [30,31]. In the case of silicas, simulations have shown the effectiveness of the MM2 forcefield [32], which was parameterized specifically for silanes and polysilanes through experimental data to reliably predict heats of formation. Whether it is the MM2, Dreiding, or UFF forcefields being used for adsorbent representations, the choice of which to use is system dependent and requires careful study. Different forcefields have been successfully used to the same end such as the parameterization of the MCM-41 adsorbent by Dreiding or by MM2 by Zhuo et al. [31] and Williams et al. [33], respectively.

In more specific cases such as functionalized surfaces or tailorable MOFs, these generic forcefields become inadequate and custom forcefields or combinations of FFs are em-

ployed [34]. Such an example is seen by Schumacher et al. [35] and Williams et al. [33] who modelled amine chains on the surface of MCM-41 using OPLS [36], the optimized potential for liquid simulations developed for proteins and incorporated into models representing water. In some instances, such as in IR-MOF-1 and Zeolitic imidazolite framework simulation studies by Babarao et al. [37] and Pellitero et al. [38], the LJ potentials were adjusted from the standard UFF values through a correction factor fitted from experiment, and their transferability ensured on similar frameworks and under different adsorbates [30,38].

In the parameterization of Carbon Dioxide gas in adsorption, EPM2 [39] is a model that is often used. Developed by Harris and Yung [39], it models the molecule through point charges and LJ parameters centred at each atom. EPM2 has been shown to predict CO_2 critical properties accurately with only a 1–2% error in liquid coexistence densities predictions. This model has been shown in several studies to accurately represent the CO_2 adsorption in Mesoporous silica adsorbents [40], Single Walled carbon nanotubes [41,42], Carbon Nanotubes [43,44], Zeolite NaY [45] silicalite (Si/Al)-based adsorbents [46], and hybrid adsorbents [47].

For methane adsorbates or methylene chains in amino-silanes, the TraPPe-UA [48] forcefield was developed specifically for alkanes to reproduce the critical properties and liquid densities through a single interaction site on the Carbon atom. The TraPPE forcefield's applications were broadened by Potoff et al. [25] to accurately model CO_2 and N_2 in a mixture with alkanes. In this model, the CO_2 quadrupole is represented similarly to the EPM2 model by a partial charge at each atomic site to represent its quadrupole moment [49]. The TraPPE forcefield has also been optimized for Nitrogen through a 3-site representation and is commonly employed for CO_2/N_2 mixtures for a variety of adsorbent and functional group interactions [49–53].

These forcefields have standardized LJ potentials in molecular simulation. Although with certain limitations, a creative approach to adapting them to each unique system has been proven and becomes an important part of employing them within the broader context of MM simulations.

2.1.3. Monte Carlo

Monte Carlo (MC) methods are statistical methods used by a variety of disciplines to tackle complex deterministic problems. In essence, MC methods rely on random sampling of a system in order to solve the thermodynamic equations of its components. The metropolis method introduced in 1953 was the first computational application of MC in the determination of the properties of an interacting system [54]. When applied to equilibrium systems, MC calculations are based on the choice of an ensemble that holds certain thermodynamic properties constant to determine the remaining properties of a system at these given conditions. The following thermodynamic relationship applies: The ensemble chosen determines the fluctuating variables of the system and an integration across the finite possibilities over a system's probability distribution will provide the average properties of a system [55]. Coinciding with this is an assigned value for the number of cycles of repeated calculations that determine the density of system sampling, the higher the number of repeated probabilistic calculations, the lower the standard deviation becomes, and more accurate results outputted (Figure 1).

The choice of calculation ensemble is specific to each topic studied, and in the case of adsorption, Grand Canonical Monte Carlo (GCMC) is the most effective in simulating adsorption isotherms and therefore will be the focus of this section. The GCMC ensemble, also known as the μVT ensemble, holds the chemical potential (μ), volume, and temperature constant while fluctuating the energy and number of molecules at thermal equilibrium. The chemical potential is related to the fugacity of the adsorbate components and is derived from it. The ensemble is applicable to a unit cell input dictated by the framework of the system, while the thermodynamic limitations apply to both the framework and the adsorbate components. Figure 2 illustrates as an example the unit cell of a mesoporous

silica structure, and the periodic boundaries applied to it in GCMC calculations to simulate the full adsorbent structure observed experimentally.

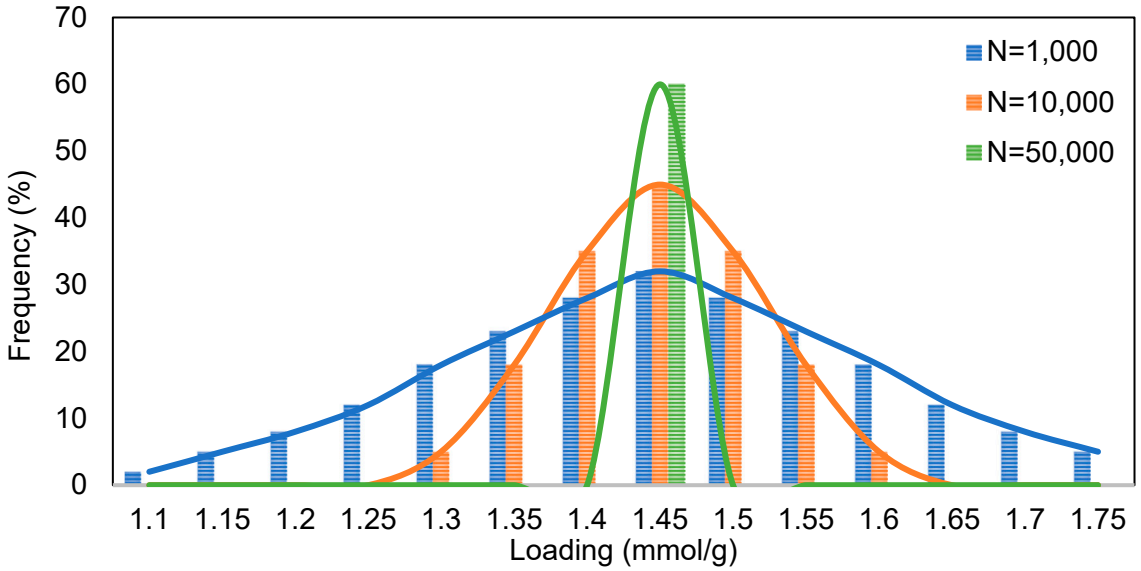


Figure 1. Monte Carlo probability distribution of a hypothetical adsorbent loading based on the frequency of sampling represented by N. The line follows the trend of each probability distribution.

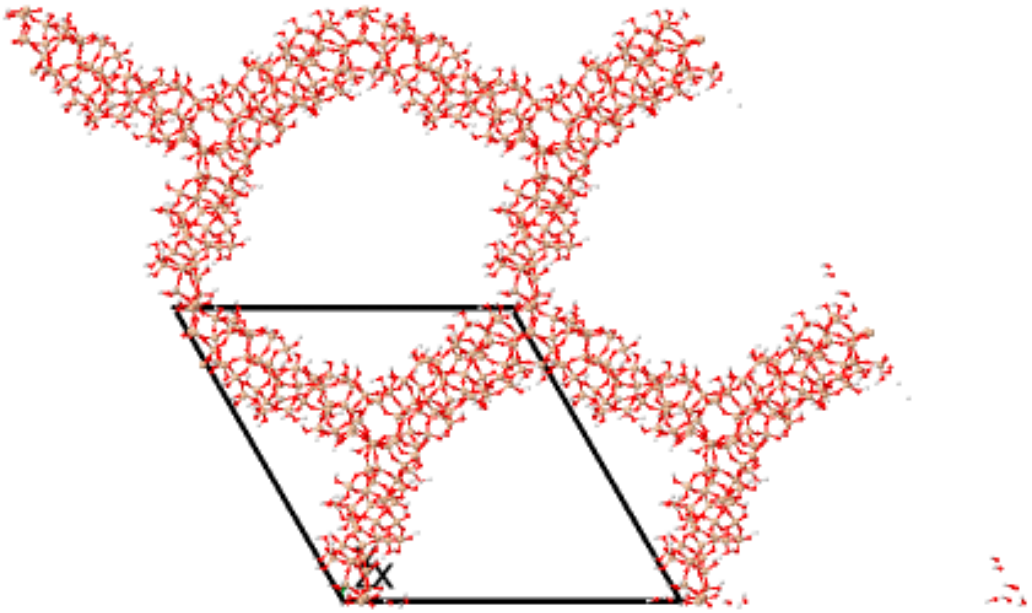


Figure 2. Mesoporous silica MCM-41 Unit Cell and periodic structure visualization for GCMC calculations [56]. '*Reprinted from Ref. [56]*'.

Once the process variables are set and held constant, a Monte Carlo software applies prespecified moves for each component within the system, such as insertion/deletion, translation, and rotation, an example is presented in Figure 3. Each move is accepted or rejected based on a program's acceptance rules, while the user-specified total number of cycles determine the accuracy. The higher the level of sampling, the more accurate and repeatable the simulation results become [57].

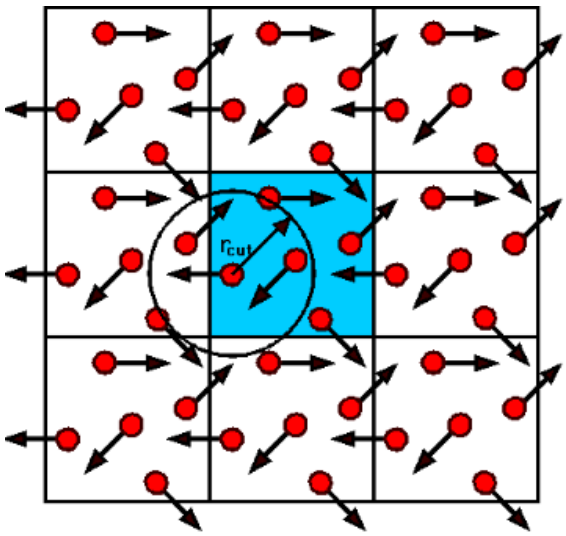


Figure 3. Periodic boundary conditions as applied to component translation moves [58]. The red circle represents an example molecule, while the arrows are the possible movements as implemented by GCMC software within the periodic boundary (In blue). '*Reprinted from Ref. [58]*'.

2.2. Quantum Mechanics

Considering the limitations of MM, Quantum chemistry addresses this by describing electron distributions and particle motions through Schrödinger's equation, also known as the wave function, which theoretically solves to a probability of finding a particle in a point in space [59].

$$\mathcal{H}\Psi_i = E_i\Psi_i \tag{12}$$

where $\mathcal{H}$ is Hamiltonian operator, Ψ_i is the wave function corresponding to the ith electronic state and E_i is the energy of the ith electronic state. In order to calculate energy and other related properties of compounds, this equation must be solved. The exact solution of the equation only possible for helium atom or for H_2^+ molecule and for other molecules the approximate methods must be used. In general, there are three approximate methods to solve the Schrödinger's equation as follow [60]:

- Ab initio (first principle) methods—Apply various approximations using wave functions to describe atomic orbitals and thus calculate properties at a molecular level.
- Semi-empirical methods—Apply a similar method to Ab Initio, but only for valence electrons.
- This type of calculation can be done using commercial programs such as Gaussian [61] or using free programs, such as MOPAC [62], MultiWFN, GAMESS [63].
- Density functional theory (DFT) methods—Identify the properties of the system using calculations relevant to the electron density of the system.

The complexity of solving the wave function led to the use of Density Functional Theory or DFT, a method based on the Kohn–Sham equation which simplifies the Schrodinger wave equation through a simulated non-interacting electron representation of a given system. This system solves to the same density of an interacting system solving for a probability density distribution of the system. As the Schrodinger wave function is a many-body problem and an N-dimension equation with three dimensions for each electron within the system, the computational power necessary for a system of more than a few atoms is at a level beyond realistic computational power [64].

With the introduction of the Hohenberg and Kohn theorem [65] (1964) and the KS equation in 1965 [66], it allowed the reduction of the 3N functions of Equation (13) below based on the spatial coordinates of each particle and its spin [$\Psi(r1, r2, \ldots rN, t)$], to be defined by only $\Psi(n(r))$, with $n(r)$ representing the electron density [67]. Equation (13) breaks down the variables involved in calculating the ground state energy, the first term

represents the electron kinetic energies, $V(r)$ describes electron–nuclei interactions, $V_H(r)$ describes electron–electron coulomb repulsions, and $V_{XC}(r)$ is the exchange correlation which includes all additional interaction forces and whose approximated form or value dictates the accuracy of the DFT calculation [68].

$$\left[\hat{T} + \hat{V} + \hat{U}\right]\Psi = \mathrm{E}\Psi \tag{13}$$

$$\left[-\frac{h^2}{2m}\nabla^2 + V(r) + V_H(r) + V_{XC}(r)\right]\psi_i(r) = \varepsilon_i\psi_i(r) \tag{14}$$

where $\hat{T}$ is the Kinetic energy, $\hat{V}$ is the external potential (from atomic nuclei), $\hat{U}$ is the electron-electron interaction energy, E is the energy.

As DFT relies on mathematical short-cuts, the ground-state energies calculated are inherently uncertain, and there is currently no clear method of calculating the magnitude of this deviation. This is carried over to excited state energies from DFT calculations, and they are considered even less accurate compared to ground-state energy calculations [64]. MP2 calculations can be employed to offer the highest level of accuracy for describing dispersion energies, but they are significantly more computationally expensive [9]. In addition, VdW interactions are not accounted for in DFT functionals, and must be incorporated into hybrid DFT calculations. Rana et al. [69] developed such functionals for CO_2 adsorption in MOFs, where they showed higher level of accuracy in CO_2-binding enthalpies, although a trade-off was made with a decreased accuracy in predictions of metal-CO_2 bond length [70].

As for the general considerations in DFT, computational limitations for large systems lead to simulation models that only address single adsorbate or surface group interactions with the adsorbent surface. With respect to amine functionalization, this treatment requires detailed knowledge of the possible species existing before, during, and after adsorption. Narrowing down the state of each molecule that could exist at a certain point adds to the complexity of DFT applications. In general, the choice of functional, basis set and system size for DFT calculations is a science in itself, and a trade-off between calculation accuracy and computational cost is always present [21,64,71].

3. Applications of Computational Chemistry on Mesoporous Silica Adsorbents

3.1. MCM-41, SBA-15 and MCM-48—A Class of Mesoporous Silica

Mesoporous silica adsorbents have been extensively studied experimentally for their simple modification and high amine-loading capacity as a result of their large surface area and pore volume [72,73]. There are an abundance of studies utilizing simulation software for deeper insight into the adsorption mechanism of mesoporous silica, but the methodologies used vary depending on the author and study criteria. Some of the selected studies within the literature have been listed in Table 2.

Most studies target a deeper understanding of adsorption of CO_2 in flue gas. A few explore the effect of amine functionalities on the adsorbate–adsorbent interactions and are discussed in detail in Section 3.2. The major consideration between these two applications is physical adsorption (physisorption) or chemical adsorption (chemisorption) of the target species. Physisorption refers to adsorption through physical forces, such as van der Waals forces. Comparatively, chemisorption refers to adsorption by bond formation, such as covalent chemical bonds [74,75]. Identifying the adsorption phenomena taking place is essential when choosing the simulation medium and method, as some numerical simulation methods cannot mimic real-world chemical reactions.

Table 2. Summary of studies on MCM-41/SBA-15 applications for carbon capture.

Adsorbent	Structure Construction	Functionality	Chemisorption	Scope	Structure and Adsorption Validation	Refs.
MCM-41	Cylindrical pores in an amorphous silica Unit Cell. UFF Geometry optimization. BET = 983.4 m^2/g	Grafted AP on the surface with energy bias for grafting sites. Monodentate bonding with the surface was used. Coupled-decoupled configurational bias to allow amine movement during grafting.	Modelled with a fixed pre-simulation minimum value of chemisorbed CO_2 and carbamate formation.	Physisorption interactions increase with functionalization even as pore space decreases. Differences in experimental and simulation results at low pressures.	N_2 isotherm at 77K—Small discrepancy at low pressure possibly because of a smaller simulation size compared to experimental. CO_2 at 263K up to 20 bars— Matched very well at higher pressures with experimental data.	Builes et al. [52]
MCM-41	Cylindrical pores in an amorphous silica UC. BET = 1161 m^2/g	None	N/A	Two models with radius of 19 and 17 Å With BET equivalent to experimental MCM-41 studied. −OH branches at 5.38–5.85 OH/nm^2. CO_2 adsorption simulated its dependency on the surface functional groups. N_2 adsorption simulated its dependency on pore volume.	Validated through comparison with experimental data. Added a correction coefficient based on structural differences to validate simulation XRD patterns validated with experimental.	Jing et al. [76]
MCM-41	Cylindrical pores in an amorphous silica UC. BET = 1047 m^2/g	None	N/A	The rough surface of the adsorbent provides hydroxyl groups and defects that work as active sites for adsorption. Simulation slightly higher than experimental at high pressures.	Validated through comparison with experimental data.	Zhuo et al. [31]
MCM-41	Cylindrical pore in an amorphous silica UC. BET = 1047 m^2/g	8, 12, 16, and 24% amine coverage.	Simulated it using a strong physisorption interaction energy derived from the reaction to form carbamate.	Shown that higher grafting increases interaction with CO_2 although less adsorbent active sites are available. The adsorption of CO_2/N_2 showed a decreasing selectivity of CO_2/N_2 attributed to enhanced packing effects for N_2.	Validated through comparison with experimental data.	Zhu et al. [51]

Table 2. *Cont.*

Adsorbent	Structure Construction	Functionality	Chemisorption	Scope	Structure and Adsorption Validation	Refs.
MCM-41	Kinetic Monte-Carlo (kMC) used for structure. Organic molecules randomly introduced for functionalization and then swapped through Monte-Carlo to ensure lowest energy configurations	Variety of functional groups were tested in this study. Aminopropyl functionalized MCM-41 and phenyl-MCM-41 explicitly compared	Ignored chemisorption and studies concentrated on Pressures above 1 bar (values in which physisorption dominates). Validated using high-pressure region for Propylamine functionalized MCM-41	Higher pressure results were predictive. Showed: (1) cooperative effects between neighbouring amines, and polarity influences by amine moieties on physisorption at higher pressures (2) The positive effect of aromatic rings in avoiding hydrogen bond formation between the amine and the adsorbent surface. (Which may decrease active sites)	Validated through comparison with experimental data. Higher densities of amines did not match experimental since chemisorption was not considered.	Williams and Schumacher et al. [33,35,77].
SBA-15	The structure's pore diameter was set at 35 Angstrom as well, lower than typical SBA-15.	None	N/A	Effect of moisture on the adsorption and diffusion of CO_2/CH_4 was studied. Mapped the movement of water clusters within the pores and identified a dense water layer along the pore walls that may be formed regardless of pressure.	Validated through comparison with experimental data within literature.	Sizova et al. [78]
Hybrid MCM-41 (Confined solvent)	Cylindrical pore in an amorphous silica UC carved independently of the confined solvent. GCMC is used to fill the pores with the solvent. Solvent: octamethylcyclotetrasiloxane [OMCTS])	None	N/A	Studied CO_2 solubility in hybrid MCM-41, summarized by the effect of solvent size on the adsorbed CO_2 density profile. An analysis of the location of CO_2 molecules adsorbed as a function of solvent size was carried out.	Validated through comparison with experimental data.	Ho et al. [40]

3.1.1. Forcefield Selection

As the choice of forcefield is one of the major decisions in molecular simulations, there has been research that targets an understanding of the ideal LJ parameter values to approximate interaction energies for more accurate simulations. Emami et al. [24] developed ideal LJ parameters, bond length, and partial charges for amorphous silica nanoparticles accurately reproducing bulk and interfacial properties, allowing their incorporation into common forcefields for biomolecules and materials. However, these values are not tailored for gas adsorption systems, and exclude interactions that play an important part in mesoporous silica's gas adsorption capacity. When modelling mesoporous silicas, the choice of forcefield will depend on the choices made on the construction of the adsorbent. For example, some considerations include whether O-H has been included on the surface of these mesoporous silicas, or whether an amorphous silica matrix has been used as a skeleton.

For mesoporous silica, LJ parameters chosen to represent the framework and simulate experimental isotherms usually coincide with the well-known Dreiding generic forcefield or the MM2 forcefield. When the structure is simplified to only oxygen atoms, researchers have opted for the MM2 forcefield. Alternatively, when an amorphous silica matrix is used as a base, the Dreiding forcefield is utilized. In both cases, their values are at times fine-tuned on a per study basis to ensure the experimental and simulated isotherm match. This is also used to decide on the atom charges to be used for the simulation, which has a large variation within the literature. A table summarizing the various studies and their choice of LJ parameters and charges can be found in the supporting information.

3.1.2. Surface Structure Conception

MCM-41, introduced by Beck et al. [79] from the Mobil Research group, represent a class of adsorbents characterized as mesoporous molecular sieve types with pore diameters above 2 nm, a high surface area and a uniform distribution. Their significance stems from their inherently tailorable properties of pore diameter and pore volume with respect to the synthesis surfactants. This has popularized them for their potential use in a wide variety of applications including CCS, and gave rise to the novel synthesis of the similarly structured and tailorable mesoporous silica adsorbents, MCM- 48 [80] and SBA-15 [81].

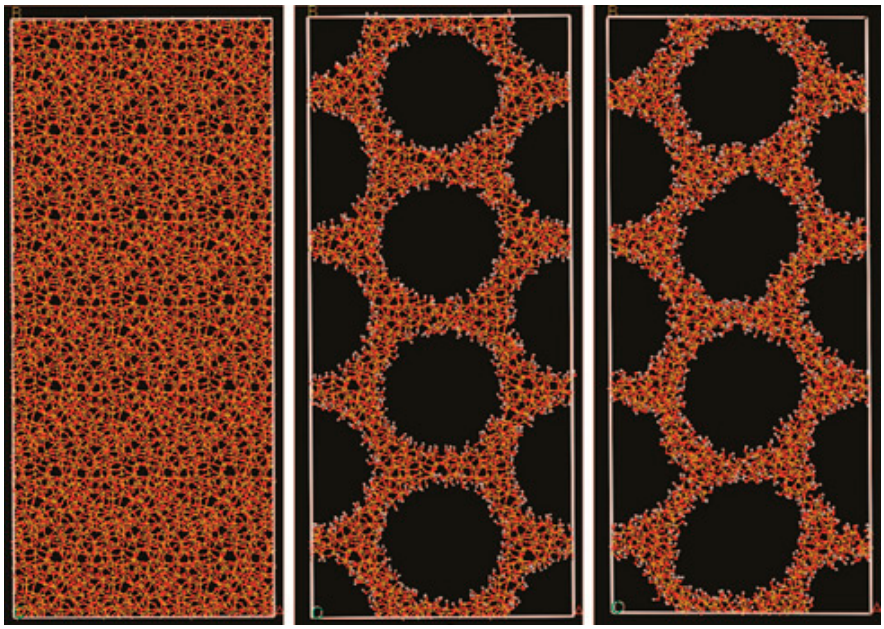
Although a pore distribution across a range of pore diameters is observed in mesoporous silicas [79,81], their characterization through Nitrogen adsorption allows for accurate measurement of mesoporous silica's pore diameters distribution, with the pronounced peak around the primary pore diameter [82]. The preparation of a simulation unit cell replicating the structure of MCM-41, MCM-48, and SBA-15 has been carried out in a variety of methods and successfully shown to mimic experimental gas adsorption tests, under certain process conditions. It is important to note the challenges associated with preparing a unit cell with the large pore diameters associated with these adsorbents. At pore diameters above 4 nm, the number of atoms within a unit cell can exceed over 1000 leading to computational issues in rendering the structure for visualization with open-source software such as Avogadro [83]. Software such as VMD [84] are designed to analyse large biomolecules and therefore are efficient in rendering a high quantity of atoms, but are not compatible with periodic crystal structural files limiting their potential to be fully used for structural preparation.

The remaining subsections separate the different methodologies employed in applying GCMC to these silicas; each subsection highlights the techniques used to build the structure, the associated forcefield parameters chosen, and the results gathered to validate and produce valuable data to compliment experimental results.

3.1.3. Amorphous Silica Matrix and Dreiding FF

The pore diameter distribution of MCM-41 was used by Zhuo et al. [31] to prepare an MCM-41 adsorbent model from a pre-set crystal database structure of amorphous silica with cylindrical pores carved into it (Figure 4). The pore diameter was set at 14.38 Ang with

a Connolly surface of 1047 m^2/g and a surface density of hydroxyl groups at 7–8 OH/nm^2. They compared the simulation to the experimental sample of MCM-41 with a BET of 1013.7 m^2/g and radius of 13.48 Ang. Experimental studies by Landmesser et al. [85] designated a value of 4.43 mmol/g to hydroxyl groups in hydrated MCM-41 adsorbent, which coincides to 2.63 OH/nm^2 in the aforementioned sample. This experimental value can be considered reasonable as Van der Voort et al. [86] demonstrated the presence of a maximum of 1.7 OH/nm^2 of free hydroxyl groups with a total of 5 OH/nm^2 of both bridged and free hydroxyl groups on silica gel. In the study by Zhuo et al. [31], they allocated Dreiding forcefield parameters for LJ potentials as well as partial charges for the Silica, Oxygen, and Hydrogen framework atoms. The charge distribution was calculated by DFT geometric optimization followed by the Electrostatic Potential (ESP) method on three different clusters of amorphous Silica (Figure 5). The simulation isotherms agreed with experimental results for both CO_2 and N_2, giving insight into the adsorbate distribution of CO_2 and selectivity of CO_2 to N_2 across a range of temperatures.



(**a**) (**b**) (**c**)

Figure 4. Steps in the construction of the MCM-41 model—(**a**) Amorphous Silica. (**b**) Carving Cylindrical Pores. (**c**) Post-geometric optimization by MM [31]. '*Reprinted (adapted) with permission from [31]. Copyright 2008 American Chemical Society*'.

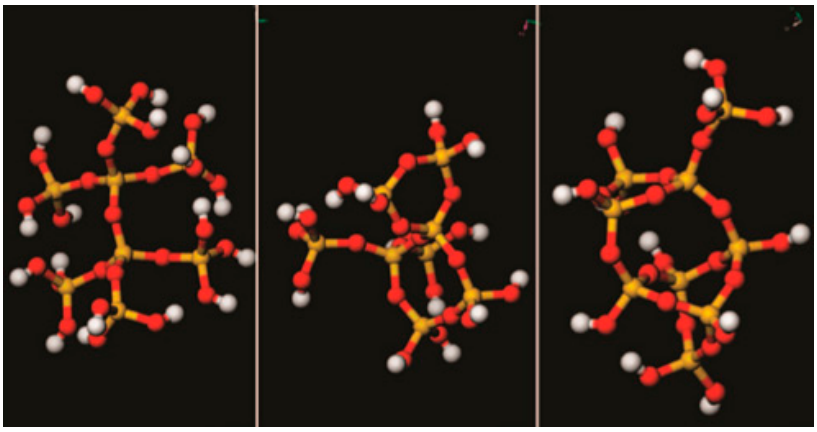


Figure 5. Three different Amorphous Silica clusters used for ESP partial charge determination [31]. '*Reprinted (adapted) with permission from [31]. Copyright 2008 American Chemical Society*'.

The parameters presented in the study by Zhuo et al. [31] are seen repeatedly used in subsequent MCM-41 studies by Jing et al. [76], Ngoc Ho et al. [40], Zhu et al. [51], and Chang et al. [87]. Although with hydroxyl groups higher than experimentally studied, the treatment of the structure and the allocation of partial charges through ESP proved adequate in recreating gas isotherms for several studies within a reasonable error, as in the study by Jing et al. [76] a correction factor was included to match experimental results.

3.1.4. Core Structure and Oxygen Contributions

In comparison to the method for structural preparation presented in Section 3.1.3, Yun et al. [88,89] suggested the assignment of LJ parameters for only the oxygen atom within the structure, with no Coulombic effects considered. This method referred to a study by Bezus et al. [90] in 1978 which assumes the adsorbate–adsorbent interactions of the structure are represented by the oxygen only. This claim is attributed to the dependence of the polarizability of oxygen on the Si/Al ratio in a zeolite, making their contribution negligible, and due to the surface coverage of the structure with oxygen.

In the above model, Yun et al. [89] accurately re-created adsorption isotherms across a range of temperatures of pure methane, while predications for ethane had a larger margin of error as temperatures increased, although they remained within an 'acceptable' range. The applicability of the simple model is only accurate at higher pressures, due to the simplification of the heterogeneity of experimentally synthesized MCM-41 to only an oxygen surface (Figure 6) and can be seen in the pressure range between 0–250 kpa of Figure 7. These results echoed the study by Maddox et al. [91] which had previously shown the inadequacy of a simple model in recreating low-pressure nitrogen isotherms, but also its effectiveness at higher pressures due to multilayer adsorption as the interactions of the gas shift from the adsorbent surface to the adsorbate layer.

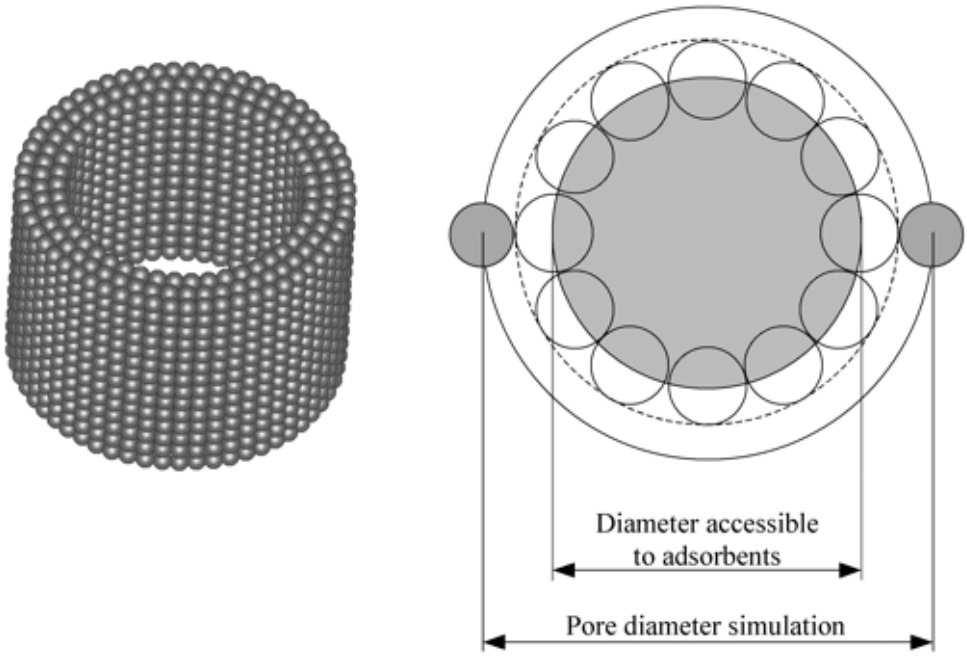


Figure 6. Yun et al.'s model of MCM-41, with the structure composed of only oxygen atoms [89]. '*Reprinted (adapted) with permission from [89]. Copyright 2002 American Chemical Society*'.

The construction and validation of the model by Yun et al. [88,89] is important as a similar methodology that includes Coulombic effects was used for CO_2 adsorption studies by Schumacher et al. [35,77,92], and Williams et al. [33] modelling surface-group-modified MCM-41 and will be discussed in Section 3.2. Additionally, the allocation of LJ parameters to only oxygen for MCM-41 was repeated by C. Williams et al. [93] for a silica matrix prepared through MD methods utilizing melt-quench techniques. This method mapped an

automated procedure to prepare an MCM-41 structure of varying wall thickness and pore diameter and validated it through experimental results. Their results showed variations at higher pressures but at lower pressures accurate isosteric heats and loading data were collected for CO_2.

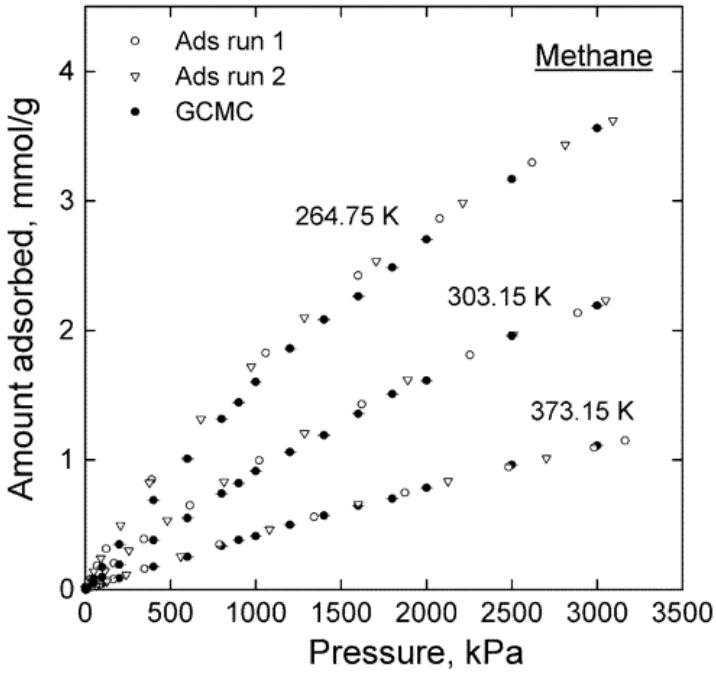


Figure 7. Comparison of experimental and simulated Methane pure component Isotherms [89]. '*Reprinted (adapted) with permission from [89]. Copyright 2002 American Chemical Society*'.

3.1.5. Cristoballite Matrix, Surface Roughness and the MM2 Force Field

He and Seaton [94] demonstrated the important role surface heterogeneity plays in adsorption of CO_2 at lower pressures by modelling MCM-41 with only oxygen LJ contributions but including Silica atoms in the structure and assigning partial charges to them without LJ parameters. Their findings in combination with studies by Coasne and Pellenq [95] were developed on by Sizova et al. [78] in adsorption studies of CO_2/CH_4 and CO_2/N_2 on SBA-15 with respect to moisture effects on the interaction mechanism. The structure used was p-cristoballite for the skeletal model, and random movements were imposed on the atoms to re-create the amorphous quality of SBA-15 with a cylindrical pore carved through the centre. In this study, the pore diameter of SBA-15 was modelled as smaller than typical experimental data, but they concentrated on the effect of water on adsorption and therefore only validated the water-adsorbent interactions. This provided key information on the molecular wall formed by water on SBA-15 blocking CO_2 adsorption.

3.1.6. Structural Design for Alternative Applications

To accurately target a structure that replicates the exact internal morphology of MCM-41 and SBA-15, Battacharya et al. [96] developed a method through the reproduction of synthesis procedure involving template removal through configurational bias Monte Carlo (CBMC), thus creating an uneven surface roughness model. This method was originally developed by Pellenq and Levitz [97] using TEM data correlations to recreate the internal structure of mesoporous adsorbents, further applied to MCM-41 by Coasne et al. [98]. The uneven pores were imposed on a p-cristobalite crystal structure to prepare the simulation unit cell. This structure showed agreement with experimental data for Argon adsorption at 77K, but overestimated values at low to intermediate pressures and no results were reported for CO_2. In comparison to smoother surface roughness, both models exhibited

acceptable agreement with experiment, although higher surface roughness coincided with more accurate data at longer simulation cell lengths.

3.2. Surface Groups and Chemisorption

The incorporation of surface groups onto mesoporous silica substrate has been shown to significantly enhance the selectivity of the adsorbent to CO_2, as well as the total loading at a range of pressures and temperatures [99–103]. Grafted amino silanes have been shown to have realistic cyclability compared to impregnated amines onto mesoporous silica due to the covalent bonds formed with the surface [100,102,104]. Primary, Secondary, Tertiary, Diamines, and Triamines have all been deeply studied, with experimental studies showing Primary and Triamine competitively enhancing CO_2 adsorption capacity at 1 bar and temperature range between 298–343K [100,103,105,106].

However, as mentioned in Section 2.2 chemisorption cannot be directly modelled through MC or MD simulations. In order to accommodate the chemisorption of CO_2 on amines, which follows the reaction route in Equations (15) and (16) [5,107], various methods are utilized to include its contribution, and will be discussed in Section 3.2.2.

$$CO_2 + 2RNH_2 \rightarrow RNHCOO^- + RNH_3^+ \quad (15)$$

$$CO_2 + 2R_2NH_2 \rightarrow R_2NHCOO^- + R_2NH_2^+ \quad (16)$$

With DFT, computational studies simulating the chemisorption of CO_2 adsorption on functionalized mesoporous silica are possible, but an accurate representation of the adsorbent structure and functional groups will contain over 1000 atoms, and the computational cost and time is unfeasible. Consequently, DFT becomes a tool to understand single adsorbent–adsorbate interactions within the system, or to develop parameters for the system to be used in GCMC simulations.

3.2.1. DFT in Functionalized Adsorption Studies

Mafra et al. [103,108] studied the chemical species formed from CO_2 adsorption in CO_2/CH_4 mixtures on amine-functionalized SBA-15 through DFT analysis coupled with SSNR characterization. The silica surface cluster in the simulation was based on an alpha-quartz, and functional amine groups were placed on the surface to replace dangling -OH bonds. Figure 8 shows an example of the model for Primary amine (APTES) used on the studied surface.

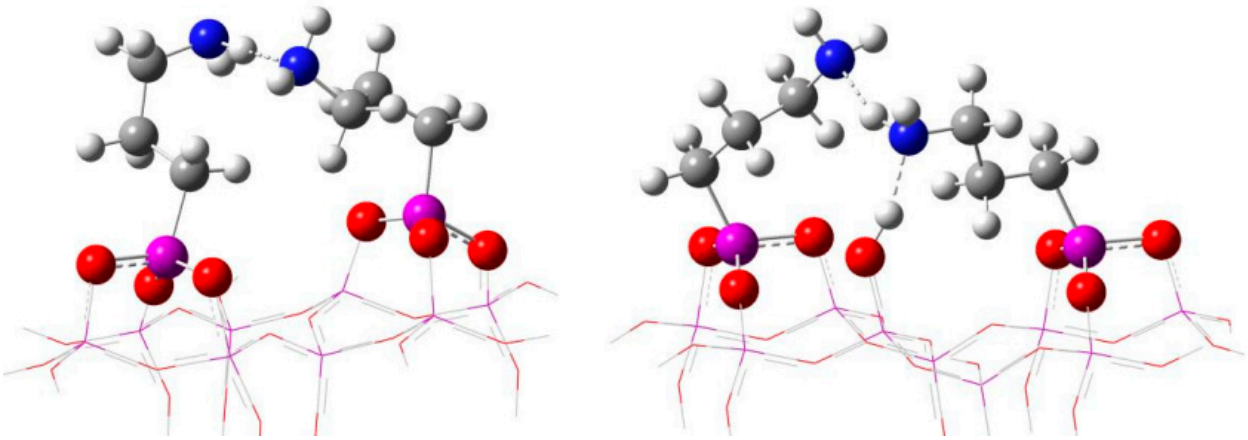


Figure 8. APTES-modified silica surface post-DFT geometric optimization [103]. *'Reprinted (adapted) with permission from [103]. Copyright 2017 Elsevier B.V. All rights reserved'.*

By employing this C NMR and DFT, they narrowed down the entities of chemisorbed CO_2 species on amine moieties as a factor of the neighbouring atoms and therefore surface densities of the amines (Figure 9). The three possible species formed with APTES (primary amine) functionalized silica can be referred to in Figure 10. This multifarious method confirmed the possibility of the formation of carbamic acid moieties stabilized by Hydrogen Bonding for certain conditions, structures that had been previously thought to be unstable. This was confirmed by calculating dissociation energies and correlating them to NMR resonances under adsorption/desorption conditions; in this manner they demonstrated that the existence of these species was possible. This explained the partial reversibility of CO_2 adsorption under low pressure and provided insight on enhanced physisorption because of amine functionalization in CO_2/CH_4 applications.

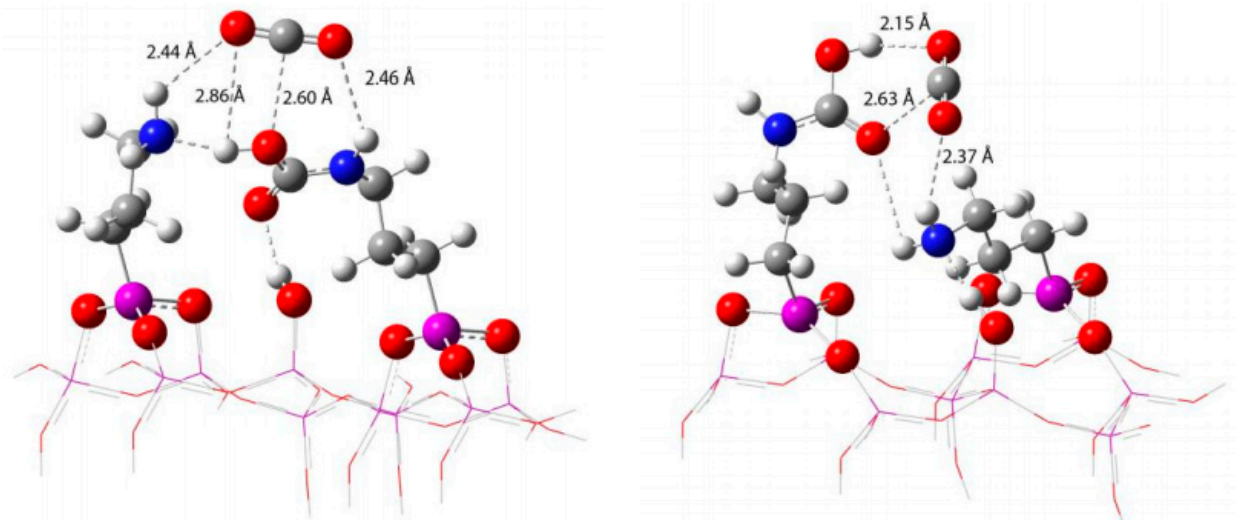


Figure 9. Interaction of physisorbed CO_2 with carbamic acid and non-reacted NH_2 moieties [103]. '*Reprinted (adapted) with permission from [103]. Copyright 2017 Elsevier B.V. All rights reserved*'.

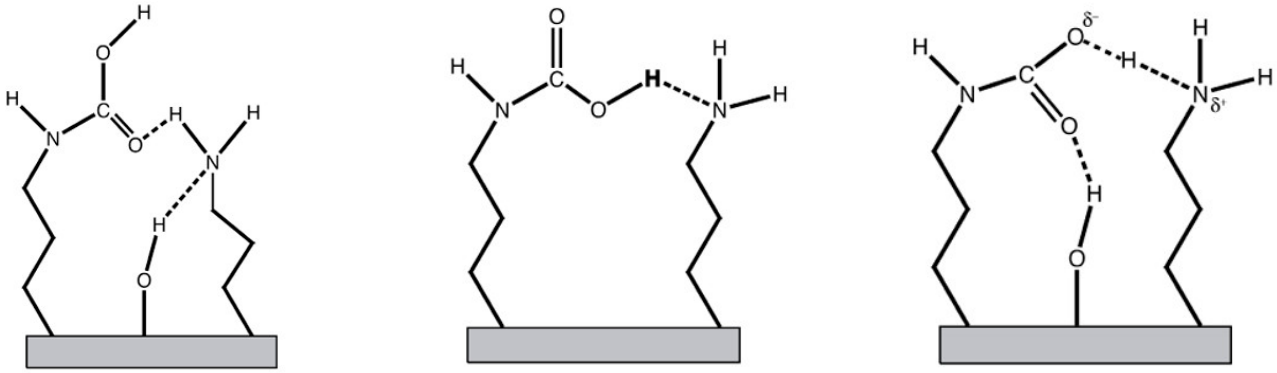


Figure 10. Structures of species formed by carbamic acid interaction with adsorbent surface and neighbouring molecules [108]. '*Reprinted (adapted) with permission from [108]. Copyright 2017 American Chemical Society*'.

3.2.2. GCMC and Modelling Simulated Chemisorption

Approaching the problem differently, Zhu et al. [51] used a combination of DFT and GCMC to simulate and study CO_2/N_2 isotherms on MCM-41 functionalized with primary amines at 8, 12, 16, and 24 wt% amine coverage. The standard LJ potential parameters for CO_2 and amine interactions were redefined to account for a stronger interaction energy

through a simple equation that accounts for all the energies of the molecules involved in the formation of carbamic acid.

$$E_{interaction} = E_{amine+CO_2} - \left(E_{amine} + E_{CO_2}\right) \quad (17)$$

The variable $E_{interaction}$ in Equation (17) is based on a straightforward DFT energy calculation for CO_2, amine, and the carbamic acid and then incorporated into the GCMC model. The rest of the system maintained a Dreiding generic potential parameters and the LB mixing rule. This method was able to accurately predict CO_2 capacity and CO_2/N_2 isotherms up to 1 bar. The simulation provided density profiles of CO_2/N_2 across the surface, mapping the active sites for CO_2 versus N2 adsorption, but the imposed interaction energy imposes a stronger physical interaction that may cast doubt on the accuracy of the atomic density profiles.

In an application to KCl surface groups adsorbing via physisorption, Kwon et al. [109] calculated the partial charges through Mullikan population analysis and applied DFT to calculate interaction energies between gas molecules and the framework surfaces of both SiO_2 and KCl functional groups. In this method, they developed an 'improved Dreiding force field' (IDFF) for the system that allowed them to validate CO_2 and CH_4 adsorption data on such a system. Such applications are a good example of the added benefit and validity of the combined use of DFT and GCMC calculations.

3.2.3. GCMC and Analysing Physisorption

The inability of modelling electron exchange by Monte Carlo simulation led to the development of a diverse set of methods to model the chemisorption of CO_2 on amine surface groups. Builes and Vega [52] completely ignored chemisorption, and specifically modelled and analysed the intra- and intermolecular interactions of carbamate moieties with pure component CO_2 gas. The amine chains were generated under a coupled–decoupled configurational bias (CDCB) algorithm to allow re-growing of amine chains thus accounting for bending/torsion contributions in the simulation.

Williams et al. [33] and Schumacher et al. [35] both concentrated only on higher pressures to better understand interactions of functional groups with CO_2. Schumacher et al. [35,92] modelled aminopropyl-modified MCM-41 for only physical interactions between CO_2 and NH_2 moieties up to 20 bar. Williams et al. [33] employed a similar procedure to investigate a multitude of surface groups with a range of functional moieties and surface coverage up to 50 bar. In both studies, only physisorption was modelled as at higher pressures it has been previously shown that in amine-functionalized adsorbents physisorption is the leading adsorption mechanism once all chemisorption sites are occupied [110,111]. The exact pressure threshold depends on the process conditions, type of amine, and surface coverage, but both studies demonstrate the transition at below 0.5 bar. Schumacher et al. [35] confirmed the validity of their model at higher pressures by comparing the experimental and simulation results of CO_2 adsorption in 10% AP-functionalized MCM-41 (Figure 11). On sampling a multitude of functional groups, they concluded that an amine surface group containing an aromatic ring such as diaminophenyl (Figure 12a) would be the optimal functional group for CO_2/N_2 applications. This was a result of two things: (1) Projecting the amine moieties or polar groups into the pore space enhances selectivity. (2) The formation of hydrogen bonds between the surface groups and the adsorbent surface can decrease adsorption sites for CO_2.

Through GCMC, Williams et al. [33] gathered CO_2 loading capacity and selectivity data for the functional groups, some of which are listed in Figure 12a–d, at surface coverages of 25%, 50%, 75%, and 100%. Table 3 can be referred to for an example of the sampling results for CO_2/N_2 selectivity by their group. In this extensive analysis of surface groups, hexaminoterphenyl (Figure 13) modified MCM-41 showed competitive selectivity to SAPO-34, and zeolite Y, with a type I isotherm ideal for PSA applications, and enhanced capacity appreciably compared to raw MCM-41.

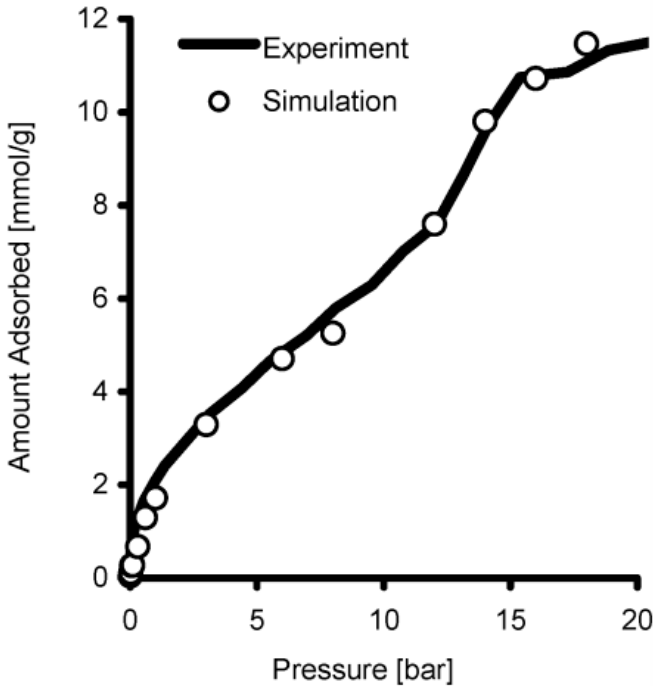
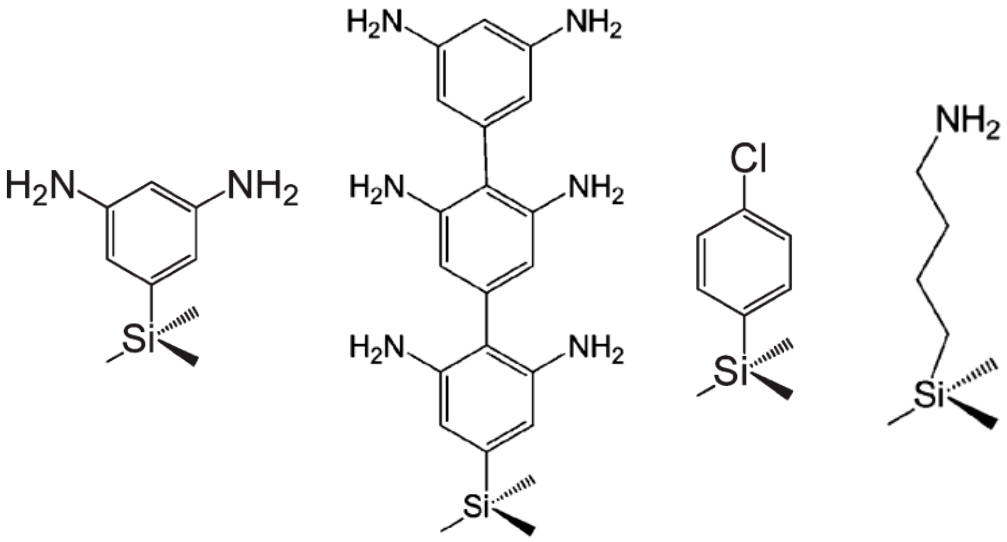


Figure 11. CO_2 Isotherm on Aminopropyl-modified MCM-41. 263K, AP:Si = 0.1. *'Reproduced with permission from Springer Nature' [35].*



(**a**) (**b**) (**c**) (**d**)

Figure 12. Structure of (**a**) Diaminophenyl with silanol bond, (**b**) Hexaminoterphenyl, (**c**) Chlorophenyl, (**d**) Butylamine.

As such, the benefits of screening functional groups on mesoporous silica through molecular simulation are quite clear, allowing for quick validation of potential structures in carbon capture applications. Additionally, the coupling of experimental analysis methods with DFT in surmising reaction intermediates is beneficial. The studies discussed in this section use different methodology for the development of the model structure and parametrization of the system yet are all able to satisfactorily simulate experimental isotherms, within certain constraints. Nonetheless, care must thus be taken in defining the system that will be studied and the limitations inherent. For example, choosing an ideal method to model chemisorption, which may include:

(1) Adding a Correction factor
(2) Describing it as a strong physisorption energy
(3) Highlighting regions in which chemisorption is negligible.

There is benefit in gas adsorption analysis through Molecular Simulation but understanding the limitations of the simulation methods is crucial in ensuring that this method of data collection is appropriate.

Table 3. Simulated selectivity of CO_2/N_2 mixture on MCM-41 functionalized with 50% coverage of listed surface groups at 1 and 10 bar at 298K [33].

	Pore Diameter = 4.2 nm		**Pore Diameter = 1.9 nm**	
	1 bar	**10 bar**	**1 bar**	**10 bar**
unmodified MCM-41	7.0	6.4	9.0	8.5
difluorophenyl	12.3	8.9	12.7	12.8
diaminophenyl	16.5	13.9	16.9	18.0
propylamine	8.7	7.2	10.0	9.3

4. Application of Computational Chemistry for Carbon-Based Adsorbents

Carbon-based adsorbents range from commercially available activated carbon materials, with high surface areas reaching up to 3000 m^2/g, to Carbon Nanotubes commonly studied for Coal Bed Methane Extraction and CO_2 storage [112]. Modifying CNTs with amines has also been shown to perform better by Lu et al. [113] in certain conditions. Activated Carbon derived from different certain biomass, has been demonstrated to have a CO_2 loading capacity at high pressures comparable to zeolites and MOFs, while maintaining a high selectivity of CO_2/H_2 [114,115].

Within the context of CO_2/CH_4 adsorption, Martin et al. [116] and Plaza et al. [117] synthesized an activated carbon derived from phenolic resin and olive stone with a CO_2 capacity of 1.83 mmol/g and selectivity of 4.26 in one sample under 50%CO_2/CH_4 feed with 25C and 120 kPa adsorption conditions. In CO_2/N_2 applications, Gonzalez et al. [118] reported a 1.1 mol/g CO_2 capacity and 7:1 CO_2 selectivity under a 15% CO_2/N_2 feed at 101 kPa and 25 °C from almond-shell-derived Activated Carbon [118]. Pore morphology, internal architecture, and surface group doping of carbon adsorbents are the key factors in carbon-based adsorbent performance, and manipulating them has been shown to alter adsorption efficiency [119–123].

Although potentially effective in carbon capture, ACs are outperformed and under researched in comparison to Zeolites and MOFs, and applications of computational molecular simulations in pre- and post-combustion carbon capture using Activated Carbon are scarce in number. The majority of carbon-based adsorption applications concentrate on Supercritical CO_2 for CO_2 storage in Carbon Slit pores to better understand the surface-Adsorbate interactions in geological reservoirs such as coal beds, as well as Carbon Nanotubes for their enhanced mechanical properties [124–126]. Some studies explore a range of process conditions and results become applicable for subcritical CO_2 carbon capture, such as by Liu et al., and will therefore be discussed below. For the structural modelling of CNTs, this topic is broad and is beyond the scope of this paper, the reader can refer to the Rafee and Moghadam [14] review for further information on CNT structural preparation in molecular simulation.

4.1. Disordered Carbon–Structure Conception

Activated Carbon can be described as an amorphous structure of high porosity with pore sizes ranging from macro down to micro levels. The simulation of this disordered internal structure was addressed in a study by Davies and Seaton [127] investigating the relationship between the pore size distribution and the pore structures of AC simulation models. They found that slit-shaped pores are a representative image of the pore morphology of real AC, but that care should be taken as the average pore size would represent

the lower limit of the average pore size if no interconnections exist in the real structure. Heuchel et al. [128] built on this study by preparing a model that can use experimental pure component isotherms of CO_2 and CH_4 to fit a PSD to an experimental sample for further predictions of mixture adsorption. Although with some limitations in accurately predicting the CO_2 selectivity with pressure, it was found to successfully predict the adsorption of binary mixtures of CO_2 and CH_4, and the adsorption of their pure components at high pressures. In comparison, Farmahani et al. [129] used Hybrid Reverse Monte Carlo (HRMC), a method similar to Metropolis Monte Carlo but minimizes the error norm instead of the internal energy. In the case of their study, the error norm was based on the structure factor derived from experimental diffraction data, and through HRMC they constructed a 3-D model representative of the SiC-DC adsorbent's internal structure.

4.2. Activated Carbon and CNTs—Simulation Applications

Liu et al. [130] used the HRMC method to prepare two of the three Carbon Structures in Figure 13. They mapped the effects of pore morphology on adsorption by simulating the adsorption of a mixture of 5%, 25% and 50% CO_2/CH_4 from 300 to 350K and up to 3 MPa pressures on SiC-DC, ACF-15, and CNT (d_p = 0.81–2.03nm). For simulation parameters, the All-atom model for CH_4 was found to more accurately replicate adsorption due to its reduced value for potential energy with pore walls. Across the broad range of conditions, CO_2 selectivity was found to increase with pressure in CNTs compared to amorphous carbons. In amorphous carbons, selectivity initially decreased and had a dependency on the ratio of CO_2/CH_4 at higher pressures as can be seen in Figure 14 They attributed the CNT results to a molecular sieving effect combined with CO_2-adsorbate interactions. Comparatively, amorphous carbons with a higher number of pore widths at less than 0.4 nm but less confined pore effects, follow a sieving effect at lower pressure that rapidly reduces as CO_2-adsorbent interactions drop and are not counterbalanced by molecular sieving and CO_2-adsorbate interactions. By screening several CNT pore diameters, they concluded that for CO_2/CH_4 separation a CNT with a diameter of 0.95 nm provides enhanced capacity and selectivity compared to disordered carbons.

The validation of HRMC in reproducing the complex micro-porosity of activated carbon for accurate simulation of CO_2 adsorption opens many doors towards multivariate studies of these structures. Additionally, Liu and Bhatia [41] showed the ease of screening pore diameter sizes in concluding optimal structures for CO_2 adsorption, but this can be easily carried over for a diverse range of applications (Figure 14). This is demonstrated by the wide range of adsorption pressures tested of modified CNTs in the following section.

4.3. Surface Group Effects—CNTs

Lu et al. [44] simulated CO_2 loadings across a range of pressures from 0.1 to 100 bar on carbon foams, mesoporous carbons, and CNTs in both modified and raw forms (Figure 15). They concentrated on CNT models as they performed the best attaining high selectivity of CO_2/CH_4 balanced by high CO_2 capacity. They reported a constant CO_2 loading from 0.1 to 100 bar for carboxyl-modified CNTs. In terms of selectivity, Figure 16 shows an enhanced selectivity with CO_2/CH_4 values exponentially dropping as pressure approaches 10 bar in an equimolar mixture of CO_2 and CH_4. These results suggested a strong preferential interaction between CO_2 and the carboxyl groups up to surface saturation, with an increase in selectivity in response to temperature.

The results from the study by Lu et al. [44] show promise for carbon capture and storage applications by selective modification and tailoring of internal architecture. However, no experimental data were reported to validate the results, and further research into the feasibility and pilot-level applications in response to such functionalization is necessary. This is contrasted to experimental data for amine-functionalized carbons, such as by Chungsying Lu et al. [113] in which they demonstrated promising experimental results of amine-functionalized CNTs compared to zeolites and activated carbon at 100 kPa and 25 °C. To further build on such work, MC simulations may aid in outputting data for a

wide range of process conditions and structural modifications. Nonetheless, it is important to note the limitations of GCMC in simulating chemisorption, particularly relevant for adsorbents functionalized by amines.

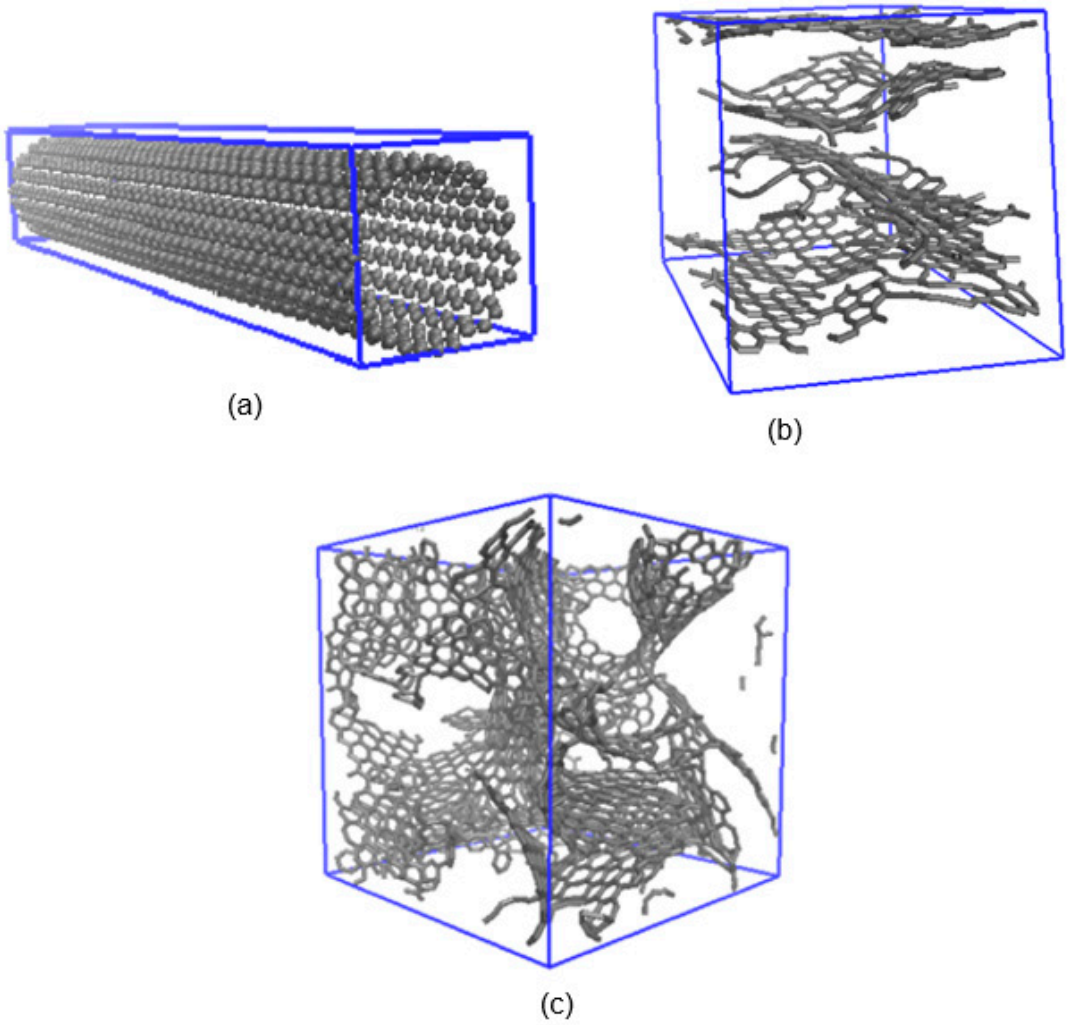


Figure 13. Simulation input for the structural framework of (**a**) CNT, (**b**) ACF-15, and (**c**) SiC-DC [130]. '*Reprinted from Ref. [130], with permission from Elsevier*'.

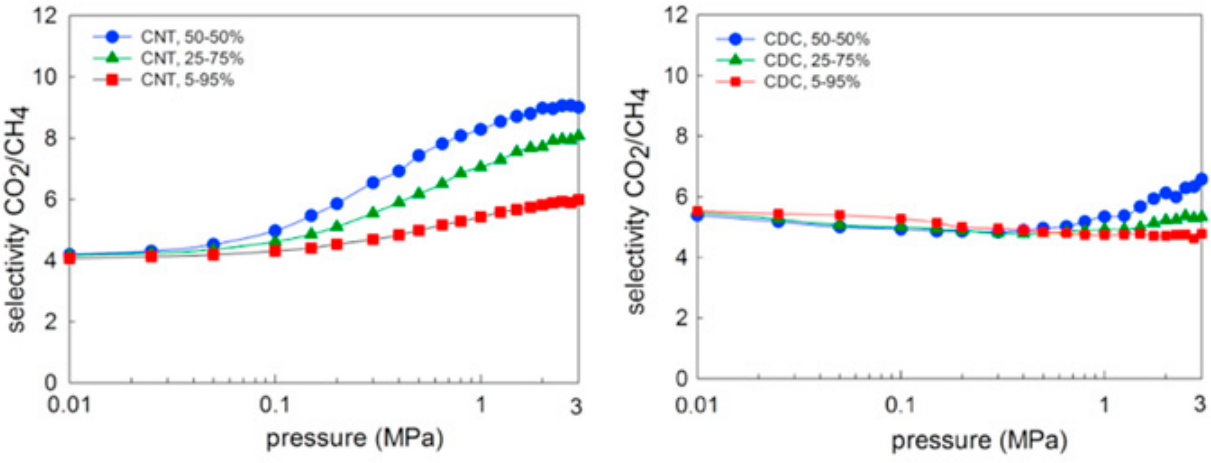


Figure 14. Selectivity of CO_2:CH_4 gases in CNT and SiC-DC at various compositions [130]. '*Reprinted from Ref. [130], with permission from Elsevier*'.

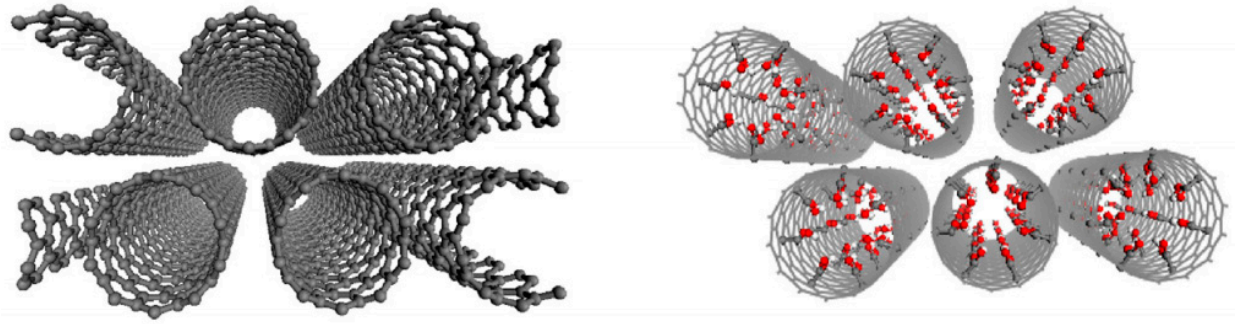


Figure 15. Simulation structure for unmodified and COOH-surface-modified CNT [44]. The red spheres represent Oxygen, white represents hydrogen, and grey represent carbon. '*Reprinted from Ref. [44], with permission from Elsevier*'.

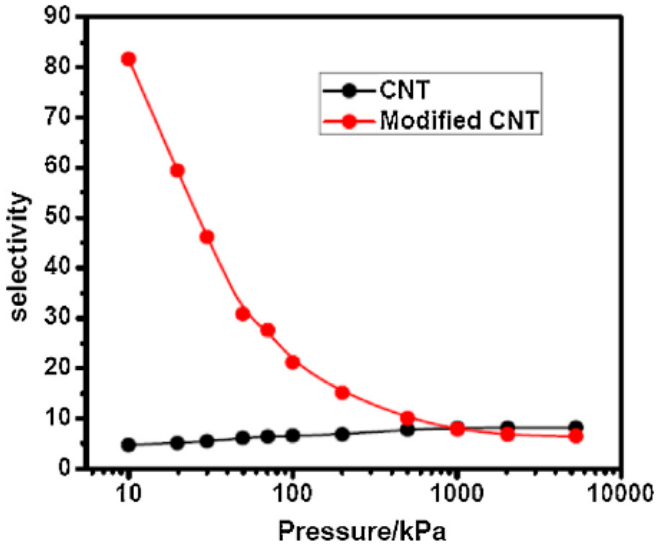


Figure 16. Simulated results for CO_2/CH_4 selectivity on modified and unmodified CNT [44]. '*Reprinted from Ref. [44], with permission from Elsevier*'.

4.4. DFT in CNTs and ACs

For carbon-based adsorbents, DFT studies have been employed not just for an understanding of chemisorption, but for system parametrization. Interaction energy provides key data for Molecular Mechanics forcefield parametrization and also validates models with calculated Heats of adsorption from experimental data.

Cinke et al. [125] in 2003 studied CO_2 adsorption in single-walled carbon nanotubes in subcritical and supercritical CO_2 conditions combining MP2 methods and experimental studies to estimate binding energies of adsorbed CO_2 on the surface of graphite and (9,0) carbon nanotubes. Previously estimated values by Zhao et al. [131] using DFT methods placed the binding energies at higher values, but Cinke et al. [125] validated the calculated heat of adsorption through their own experimental results, approximating it at 0.035 eV. The simulation provided key information of the side-on-tube orientation of CO_2 adsorption, and the physisorption-dominated adsorption at temperatures between 0–200 °C.

4.5. DFT in Functionalized CNTs and ACs

Experimentally, Chungsying Lu et al. [113] amine functionalized Granular Activated Carbons and CNTs with APTES—a primary amine often studied in silica applications. They showed a better performance in modified CNTs compared to amine-functionalized

silicas and carbons. Such studies demonstrated the potential of amine functionalization in carbon-based adsorbents.

Xiao et al. [132] studied the thermodynamics of N-substituted Graphanes in a DFT study on the alterations to interaction energy between CO_2, and surface -NCOOH and -NH_2 moieties. They found that the adsorption of CO_2 is not enhanced unless in the presence of H_2O through the formation of bicarbonate, or carbamate stabilized with nearby Hydrogen bonds. This detailed study surmised the restrictions posed by adjacent -NH_2 groups due to insufficient stabilization of formed species, and the favourable effect of neighbouring -OH groups, as has been confirmed in other DFT and experimental studies with amine-functionalized mesoporous silica [108,133]. In a most recent study that concentrated on potential for CO_2 storage and sensing, Philemon and Korir [134] surveyed the alterations to adsorption as a result of Al, B, N, and S surface binding on SWCNTs. They found that N and B doping improves CO_2 interactions because of lower adsorption energies and separation distances, while temperatures above 150 °C expelled CO_2 in N-doped SWCNTs.

Although Philemon and Korir's [134] study looked for insight on CO_2 storage and sensing, initiatives by them and Xiao et al. [132], show the strength of simulation methods as applied to functional groups on carbon-based adsorbents. In general, their work coupled by the large data sets that can be generated from MC methods provide great potential in the structured analysis of determining the optimal modifications of carbon-based adsorbents on a per application basis.

5. Novel Applications of Computational Chemistry—Polymeric Adsorbents

Polymer adsorbents have gained interest as promising adsorbents with high CO_2 selectivity. In general, polymers display high stability and resistance to moisture in combination with high selectivity and CO_2 adsorption capacity; all in combination with the ability for surface modification [116,135,136]. Due to their disordered structure, further complications arise when attempting to use molecular simulation to elucidate key interactions during adsorption.

As a result, extensive research has examined synthesis methods for polymers that minimize catalytically motivated reactions in developing economically attractive polymer sorbents (Figure 17) [137–139].

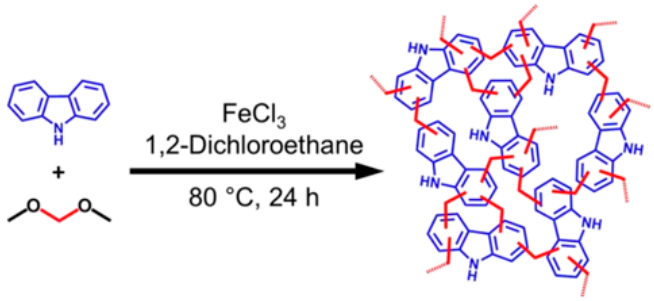


Figure 17. HCP synthesis via knitting or external crosslinking with functional group to provide enhanced adsorption performance [137]. *'Reprinted from Ref. [137]'*.

Internally, polymers are made up of complex structures and can come in a variety of configurations. This poses some challenges in realistic representations of experimental samples. However, as mentioned in Section (Carbon), HRMC was used by Farmahini et al. [129] to model the disordered internal structure of activated carbon, although not directly applicable to polymers it presents innovative approaches towards analysing amorphous internal structures. In a more direct approach, Fang et al. [140] modelled a polymer chain for gas membranes adsorption by preparing a starting polymer chain and building the membrane unit cell via the Amorphous Cell tool in the Materials Studio software (Accelrys Inc., San Diego, CA, USA), Figure 18. As polymers become further studied in carbon capture, molecular simulation techniques can build upon previous applications for well-established materials to streamline the data collection and development of these adsorbents.

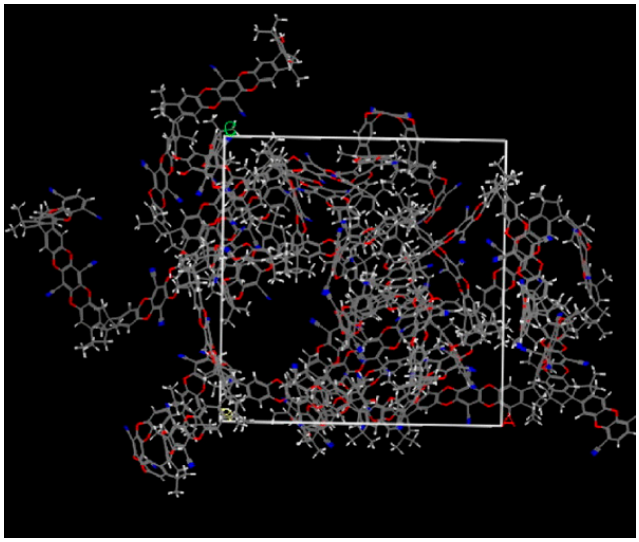


Figure 18. Polymer membrane unit cell processed through amorphous cell builder [140]. *'Reprinted from Ref. [140], with permission from Taylor & Francis Ltd.'*.

6. Intersection of Molecular Simulation and Experimental Data

Molecular simulation can help in CO_2 adsorption experiments by providing a deeper understanding of the microscopic mechanisms that govern CO_2 adsorption [141,142]. Such information can be difficult or impossible to obtain experimentally, and molecular simulation can provide a complementary approach to experimental investigations; by predicting adsorption properties of new sorbents such as predicting the adsorption isotherms [143] which describe the relationship between the concentration of CO_2 in the gas phase and the amount of CO_2 adsorbed on the surface of the adsorbent material; or by aiding in the selection of materials with high adsorption capacity and selectivity [144]. This selection can be done by predicting the adsorption behaviour of different materials for CO_2 molecules, including the equilibrium adsorption capacity, selectivity, and adsorption energy. This information can be used to screen and optimize sorbents for CO_2 capture and storage applications; by simulating the interaction of CO_2 molecules with the surface of the adsorbent material [145]. This can help researchers to identify the optimal surface chemistry and pore size distribution to maximize CO_2 adsorption. These insights can help guide the design of new materials with enhanced CO_2 adsorption properties; through interpreting experimental results by providing a molecular-level understanding of the underlying processes [146]. This information can help refine experimental protocols and improve the accuracy of experimental measurements. In a recent study Ma et al. [147], the authors prepared three porous carbon materials with different pore size distributions and heteroatom contents from biomass. They applied machine learning to study the effects of pore structure, chemical properties, and adsorption conditions on CO_2 adsorption performance based on 1594 CO_2 adsorption datasets, and to predict CO_2 adsorption capacity. The authors used molecular simulation to determine the relative significance of pore size and functional group on CO_2 adsorption under various pressures. They also discovered the mechanism of CO_2 adsorption by a single pore size and functional group species. The results of the molecular simulations supported the machine learning findings by showing that the addition of nitrogen and oxygen groups enhances CO_2 capture at relatively low pressures more so than at relatively high pressures. The results of experiments, molecular simulations and machine learning verify each other.

7. Conclusions and Future Work

This review aims to provide a wide audience with a framework for using MS methodology in gas adsorption applications. The benefits of MS span from understanding the molecular-level mechanisms of adsorption processes to generating large-simulated data

sets for adsorbent/functionality screening. This paper highlights techniques of modelling strictly on silica- and carbon-based adsorbents, although the inventive solutions used may be translated towards a variety of applications.

Current challenges in employing molecular simulation in silica- and carbon-based adsorbents include: (1) Difficulty in modelling mesoporous mediums due to the large number of framework atoms, (2) Lack of availability of optimized crystal structures for novel or niche materials, (3) Lack of standardization of forcefield parameter sets applicable to these materials, and (4) In introducing functionalities, it is difficult to scrutinize the combined contributions of chemisorption and physisorption using classical methods. Access to a multitude of open-source databases, such as the Crystallography Open Database and The Cambridge Crystallographic Data Centre (CCDC), has worked to aid in making available standardized structures and data. This promotes further collaboration between specialists and non-specialists in this field.

Additionally, when reviewing the above examples of molecular simulation in carbon capture, there is a general commonality in comparing theoretical calculations with experimental phenomena. Pore sizes, surface area and surface groups are the main structural factors used. Performance wise, the primary method of validation employs an isotherm as standard conditions, before beginning to vary additional variables through simulation. Although effective, these methods may be limited to unforeseen molecular interactions at different process conditions. This can take effect following the use of different pore size geometry, yet still reproducing the isotherm 'within reason'. Similarly, when using correction factors or employing pre-chemisorbed species on the simulation, this removes the ability to elucidate the effect of intermediates during formation. This can be overcome by combining MS techniques with experimental analytical tools, such as NMR spectroscopy, but must be approached carefully to ensure accurate correlations.

In an engineering context, investing some time in understanding the basic mechanics and applications of molecular simulations can greatly aid research initiatives in carbon capture. Through molecular simulation, a compilation of gas adsorption data across a range of pressures, temperatures, and gas compositions can be effortless (with the correct preparation). This is facilitated by a large online database of experimental data allowing for an uncomplicated validation of simulation studies. Although results might have discrepancies, such information can be a starting guide for laboratory-scale studies of potential adsorbent structures and functional groups tailored to specific operating conditions. This has already been heavily explored for screening MOF adsorbents but limited in terms of alternative adsorbent materials. Overall, future efforts should build upon a stronger communication between computational chemistry specialists and engineers to truly exploit the benefits of these simulation methods for advancing carbon capture technology towards a net-zero future.

Funding: This research received no external funding.

Conflicts of Interest: The authors declare no conflict of interest.

References

1. National for Centers Environmental Information. *State of the Climate: Global Climate Report for Annual 2019*; 2020. Available online: https://www.ncdc.noaa.gov/sotc/global/201913 (accessed on 1 March 2021).
2. Hansen, J.; Ruedy, R.; Sato, M.; Lo, K. Global surface temperature change. *Rev. Geophys.* **2010**, *48*, RG4004. [CrossRef]
3. Department for Business, Energy and Industrial Strategy. *The Climate Change Act 2008 (2050 Target Amendment) Order 2019*; Department for Business, Energy and Industrial Strategy: London, UK, 2019.
4. World Energy Balances: Overview (2019). 2019. Available online: https://www.oecd.org/publications/world-energy-balances-25186442.htm (accessed on 1 March 2020).
5. Lee, S.Y.; Park, S.J. A review on solid adsorbents for carbon dioxide capture. *J. Ind. Eng. Chem.* **2015**, *23*, 1–11. [CrossRef]
6. Abdelrasoul, A.; Zhang, H.; Cheng, C.H.; Doan, H. Applications of molecular simulations for separation and adsorption in zeolites. *Microporous Mesoporous Mater.* **2017**, *242*, 294–348. [CrossRef]

7. Farha, O.K.; Özgür Yazaydın, A.; Eryazici, I.; Malliakas, C.D.; Hauser, B.G.; Kanatzidis, M.G.; Nguyen, S.T.; Snurr, R.Q.; Hupp, J.T. De novo synthesis of a metal–organic framework material featuring ultrahigh surface area and gas storage capacities. *Nat. Chem.* **2010**, *2*, 944–948. [CrossRef]
8. Sturluson, A.; Huynh, M.T.; Kaija, A.R.; Laird, C.; Yoon, S.; Hou, F.; Feng, Z.; Wilmer, C.E.; Colón, Y.J.; Chung, Y.G. The role of molecular modelling and simulation in the discovery and deployment of metal-organic frameworks for gas storage and separation. *Mol. Simul.* **2019**, *45*, 1082–1121. [CrossRef]
9. Getman, R.B.; Bae, Y.-S.; Wilmer, C.E.; Snurr, R.Q. Review and analysis of molecular simulations of methane, hydrogen, and acetylene storage in metal–organic frameworks. *Chem. Rev.* **2012**, *112*, 703–723. [CrossRef] [PubMed]
10. Wang, H.; Qu, Z.; Yin, Y.; Bai, J.; Yu, B. Review of Molecular Simulation Method for Gas Adsorption/desorption and Diffusion in Shale Matrix. *J. Therm. Sci.* **2019**, *28*, 1–16. [CrossRef]
11. Ruipérez, F. Application of quantum chemical methods in polymer chemistry. *Int. Rev. Phys. Chem.* **2019**, *38*, 343–403. [CrossRef]
12. Ben-Mansour, R.; Habib, M.A.; Bamidele, O.E.; Basha, M.; Qasem, N.A.A.; Peedikakkal, A.; Laoui, T.; Ali, M. Carbon capture by physical adsorption: Materials, experimental investigations and numerical modeling and simulations—A review. *Appl. Energy* **2016**, *161*, 225–255. [CrossRef]
13. Li, S.; Deng, S.; Zhao, L.; Zhao, R.; Lin, M.; Du, Y.; Lian, Y. Mathematical modeling and numerical investigation of carbon capture by adsorption: Literature review and case study. *Appl. Energy* **2018**, *221*, 437–449. [CrossRef]
14. Rafiee, R.; Moghadam, R.M. On the modeling of carbon nanotubes: A critical review. *Compos. Part B Eng.* **2014**, *56*, 435–449. [CrossRef]
15. Ungerer, P.; Lachet, V.; Tavitian, B.; Applications, B.T.; Ungerer, P.; Lachet, V.; Tavitian, B. Applications of Molecular Simulation in Oil and Gas Production and Processing. *Oil Gas Sci. Technol. IFP* **2006**, *61*, 387–403. [CrossRef]
16. Salminen, P. Brownian Motion. In *Encyclopedia of Actuarial Science*; John Wiley & Sons: Hoboken, NJ, USA, 2004. [CrossRef]
17. Li, S.; Lieberzeit, P.A.; Piletsky, S.A.; Turner, A.P. (Eds.) Molecular Mechanics. In *Smart Polymer Catalysts and Tunable Catalysis*; Elsevier: Amsterdam, The Netherlands, 2019.
18. Christie, R.M. 2.9.3 Molecular Mechanics. In *Colour Chemistry*, 2nd ed.; Royal Society of Chemistry: London, UK, 2015; ISBN 978-1-84973-328-1.
19. Calvaresi, M.; Zerbetto, F. Atomistic molecular dynamics simulations reveal insights into adsorption, packing, and fluxes of molecules with carbon nanotubes. *J. Mater. Chem. A* **2014**, *2*, 12123–12135. [CrossRef]
20. Kondratyuk, N.; Nikolskiy, V.; Pavlov, D.; Stegailov, V. GPU-accelerated molecular dynamics. *Int. J. High Perform. Comput. Appl.* **2021**, *35*, 312–324. [CrossRef]
21. Monticelli, L.; Salonen, E. (Eds.) *Biomolecular Simulations: Methods and Protocols*; Humana Press: Totowa, NJ, USA, 2013; Volume 924, ISBN 9781627030175.
22. González, M.A. Force fields and molecular dynamics simulations. *École Thématique Société Française Neutron.* **2011**, *12*, 169–200. [CrossRef]
23. Frenkel, D.; Smit, B. (Eds.) Chapter 1—Introduction. In *Understanding Molecular Simulation*, 2nd ed.; Academic Press: San Diego, CA, USA, 2002; pp. 1–6. [CrossRef]
24. Emami, F.S.; Puddu, V.; Berry, R.J.; Varshney, V.; Patwardhan, S.V.; Perry, C.C.; Heinz, H. Force field and a surface model database for silica to simulate interfacial properties in atomic resolution. *Chem. Mater.* **2014**, *26*, 2647–2658. [CrossRef]
25. Potoff, J.J.; Siepmann, J.I. Vapor–liquid equilibria of mixtures containing alkanes, carbon dioxide, and nitrogen. *AIChE J.* **2001**, *47*, 1676–1682. [CrossRef]
26. Delhommelle, J.; Millié, P.; Delhommelle', J.; Millie', P. Molecular Physics Inadequacy of the Lorentz-Berthelot combining rules for accurate predictions of equilibrium properties by molecular simulation Inadequacy of the Lorentz-Berthelot combining rules for accurate predictions of equilibrium properties by mole. *Mol. Phys.* **2001**, *99*, 619–625. [CrossRef]
27. Gomez, L.F.; Zacharia, R.; Bénard, P.; Chahine, R. Simulation of binary CO_2/CH_4 mixture breakthrough profiles in mil-53 (al). *J. Nanomater.* **2015**, *2015*, 439382. [CrossRef]
28. Mayo, S.L.; Olafson, B.D.; Goddard, W.A. DREIDING: A generic force field for molecular simulations. *J. Phys. Chem.* **1990**, *94*, 8897–8909. [CrossRef]
29. Rappé, A.K.; Casewit, C.J.; Colwell, K.S.; Goddard III, W.A.; Skiff, W.M. UFF, a full periodic table force field for molecular mechanics and molecular dynamics simulations. *J. Am. Chem. Soc.* **1992**, *114*, 10024–10035. [CrossRef]
30. Moreau, F.; Da Silva, I.; Al Smail, N.H.; Easun, T.L.; Savage, M.; Godfrey, H.G.W.; Parker, S.F.; Manuel, P.; Yang, S.; Schröder, M. ARTICLE Unravelling exceptional acetylene and carbon dioxide adsorption within a tetra-amide functionalized metal-organic framework. *Nat. Commun.* **2017**, *8*, 14085. [CrossRef]
31. Zhuo, S.; Huang, Y.; Hu, J.; Liu, H.; Hu, Y.; Jiang, J. Computer simulation for adsorption of CO_2, N_2 and flue gas in a mimetic MCM-41. *J. Phys. Chem. C* **2008**, *112*, 11295–11300. [CrossRef]
32. Frierson, M.R.; Imam, M.R.; Zalkow, V.B.; Allinger, N.L. The MM2 Force Field for Silanes and Polysilanes. *J. Org. Chem.* **1988**, *53*, 5248–5258. [CrossRef]
33. Williams, J.J.; Wiersum, A.D.; Seaton, N.A.; Düren, T. Effect of Surface Group Functionalization on the CO_2/N_2 Separation Properties of MCM-41: A Grand-Canonical Monte Carlo Simulation Study. *J. Phys. Chem. C* **2010**, *114*, 18538–18547. [CrossRef]
34. Colón, Y.J.; Snurr, R.Q. High-throughput computational screening of metal–organic frameworks. *Chem. Soc. Rev.* **2014**, *43*, 5735–5749. [CrossRef]

35. Schumacher, C.; Seaton, N.A. *Modeling of Organically Functionalized Mesoporous Silicas for the Design of Adsorbents*; Springer: Berlin/Heidelberg, Germany, 2005; Volume 11.
36. Jorgensen, W.L.; Tirado-Rives, J. The OPLS Potential Functions for Proteins. Energy Minimizations for Crystals of Cyclic Peptides and Crambin. *J. Am. Chem. Soc.* **1988**, *110*, 8. [CrossRef] [PubMed]
37. Babarao, R.; Hu, Z.; Jiang, J.; Chempath, S.; Sandler, S.I. Storage and Separation of $CO_2$and CH_4 in Silicalite, C168 Schwarzite, and IRMOF-1: A Comparative Study from Monte Carlo Simulation. *Langmuir* **2007**, *23*, 659–666. [CrossRef] [PubMed]
38. Pérez-Pellitero, J.; Amrouche, H.; Siperstein, F.R.; Pirngruber, G.; Nieto-Draghi, C.; Chaplais, G.; Simon-Masseron, A.; Bazer-Bachi, D.; Peralta, D.; Bats, N. Adsorption of CO_2, CH_4, and N_2 on Zeolitic Imidazolate Frameworks: Experiments and Simulations. *Chem. A Eur. J.* **2010**, *16*, 1560–1571. [CrossRef]
39. Harris, J.G.; Yung, K.H. Carbon Dioxide's Liquid-Vapor Coexistence Curve and Critical Properties As Predicted by a Simple Molecular Model. *J. Phys. Chem.* **1995**, *99*, 12021–12024. Available online: https://pubs.acs.org/sharingguidelines (accessed on 1 June 2020). [CrossRef]
40. Ho, L.N.; Pellitero, J.P.; Porcheron, F.; Pellenq, R.J.-M. Enhanced CO_2 Solubility in Hybrid MCM-41: Molecular Simulations and Experiments. *Langmuir* **2011**, *27*, 8187–8197. [CrossRef]
41. Liu, L.; Bhatia, S.K. Molecular Simulation of CO_2 Adsorption in the Presence of Water in Single-Walled Carbon Nanotubes. *J. Phys. Chem. C* **2013**, *117*, 13479–13491. [CrossRef]
42. Skoulidas, A.I.; Sholl, D.S.; Johnson, J.K. Adsorption and diffusion of carbon dioxide and nitrogen through single-walled carbon nanotube membranes. *J. Chem. Phys.* **2006**, *124*, 54708. [CrossRef] [PubMed]
43. Huang, L.; Zhang, L.; Shao, Q.; Lu, L.; Lu, X.; Jiang, S.; Shen, W. Simulations of Binary Mixture Adsorption of Carbon Dioxide and Methane in Carbon Nanotubes: Temperature, Pressure, and Pore Size Effects. *J. Phys. Chem. C* **2007**, *111*, 11912–11920. [CrossRef]
44. Lu, L.; Wang, S.; Müller, E.A.; Cao, W.; Zhu, Y.; Lu, X.; Jackson, G. Adsorption and separation of CO_2/CH_4 mixtures using nanoporous adsorbents by molecular simulation. *Fluid Phase Equilib.* **2014**, *362*, 227–234. [CrossRef]
45. Ghoufi, A.; Gaberova, L.; Rouquerol, J.; Vincent, D.; Llewellyn, P.L.; Maurin, G. Adsorption of CO_2, CH_4 and their binary mixture in Faujasite NaY: A combination of molecular simulations with gravimetry–manometry and microcalorimetry measurements. *Microporous Mesoporous Mater.* **2009**, *119*, 117–128. [CrossRef]
46. Makrodimitris, K.; Papadopoulos, G.K.; Theodorou, D.N. Prediction of Permeation Properties of CO_2 and N_2 through Silicalite via Molecular Simulations. *J. Phys. Chem. B* **2001**, *105*, 777–788. [CrossRef]
47. Kumar, K.; Kumar, A. Enhanced CO_2Adsorption and Separation in Ionic-Liquid-Impregnated Mesoporous Silica MCM-41: A Molecular Simulation Study. *J. Phys. Chem. C* **2018**, *122*, 8216–8227. [CrossRef]
48. Martin, M.G.; Siepmann, J.I. Transferable Potentials for Phase Equilibria. 1. United-Atom Description of n-Alkanes. *J. Phys. Chem. B* **1998**, *102*, 2569–2577. [CrossRef]
49. Liu, Y.; Wilcox, J. Molecular simulation studies of CO_2 adsorption by carbon model compounds for carbon capture and sequestration applications. *Environ. Sci. Technol.* **2013**, *47*, 95–101. [CrossRef]
50. Karra, J.R.; Walton, K.S. Molecular Simulations and Experimental Studies of CO_2, CO, and N_2 Adsorption in Metal−Organic Frameworks. *J. Phys. Chem. C* **2010**, *114*, 15735–15740. [CrossRef]
51. Zhu, Y.; Zhou, J.; Hu, J.; Liu, H. The effect of grafted amine group on the adsorption of CO_2 in MCM-41: A molecular simulation. *Catal. Today* **2012**, *194*, 53–59. [CrossRef]
52. Builes, S.; Vega, L.F. Understanding CO_2 Capture in Amine-Functionalized MCM-41 by Molecular Simulation. *J. Phys. Chem. C* **2012**, *116*, 3017–3024. [CrossRef]
53. Goj, A.; Sholl, D.S.; Akten, E.D.; Kohen, D. Atomistic Simulations of CO_2 and N2 Adsorption in Silica Zeolites: The Impact of Pore Size and Shape. *J. Phys. Chem. B* **2002**, *106*, 8367–8375. [CrossRef]
54. Metropolis, N.; Rosenbluth, A.W.; Rosenbluth, M.N.; Teller, A.H.; Teller, E. Equation of State Calculations by Fast Computing Machines. *J. Chem. Phys.* **1953**, *21*, 1087–1092. [CrossRef]
55. Ungerer, P.; Tavitian, B.; Boutin, A. *Applications of Molecular Simulation in the Oil and Gas Industry: Monte Carlo Methods*; Editions Technip: Paris, France, 2005.
56. Ugliengo, P.; Sodupe, M.; Musso, F.; Bush, I.; Orlando, R.; Dovesi, R. *Coordinates of the Optimized MCM-41*; ResearchGate: Berlin, Germany, 2013.
57. Dubbeldam, D.; Torres-Knoop, A.; Walton, K.S. Monte carlo codes, tools and algorithms on the inner workings of Monte Carlo codes. *Mol. Simul.* **2013**, *39*, 1253–1292. [CrossRef]
58. Cote, A.; Smith, B.; Lindan, P. Periodic Boundary Conditions. Available online: https://www.ucl.ac.uk/~ucfbasc/Theory/pbc-mi.html (accessed on 15 June 2020).
59. Cook, D.B. 1.1 Introduction. In *Handbook of Computational Quantum Chemistry*; Dover Publications: New York, NY, USA; ISBN 978-0-486-44307-2.
60. Latour, R.A. 3.14 Molecular Simulation Methods to Investigate Protein Adsorption Behavior at the Atomic Level. *Compr. Biomater. II* **2017**, *3*, 268–294. [CrossRef]
61. Frisch, M.J.; Trucks, G.W.; Schlegel, H.B.; Scuseria, G.E.; Robb, M.A.; Cheeseman, J.R.; Scalmani, G.; Barone, V.; Petersson, G.A.; Nakatsuji, H.; et al. *Gaussian 16 Revision C. 01. 2016*; Gaussian Inc.: Wallingford, CT, USA, 2016.
62. Stewart, J. Molecular Orbital Package. 2007. Available online: http://openmopac.net/ (accessed on 23 May 2023).

63. Barca, G.M.J.; Bertoni, C.; Carrington, L.; Datta, D.; De Silva, N.; Deustua, J.E.; Fedorov, D.G.; Gour, J.R.; Gunina, A.O.; Guidez, E.; et al. Recent developments in the general atomic and molecular electronic structure system. *J. Chem. Phys.* **2020**, *152*, 154102. [CrossRef]
64. Sholl, D.; Steckel, J.A. *Density Functional Theory: A Practical Introduction*; John Wiley & Sons: Hoboken, NJ, USA, 2011; ISBN 1118211049.
65. Hohenberg, P.; Kohn, W. Inhomogeneous electron gas. *Phys. Rev.* **1964**, *136*, B864. [CrossRef]
66. Kohn, W.; Sham, L.J. Self-consistent equations including exchange and correlation effects. *Phys. Rev.* **1965**, *140*, A1133. [CrossRef]
67. Giustino, F. *Materials Modelling Using Density Functional Theory: Properties and Predictions*; Oxford University Press: Oxford, UK, 2014; ISBN 0199662436.
68. Cabeza, L.F. Advances in thermal energy storage systems: Methods and applications. In *Advances in Thermal Energy Storage Systems*; Elsevier: Amsterdam, The Netherlands, 2014; pp. 37–54.
69. Rana, M.K.; Koh, H.S.; Hwang, J.; Siegel, D.J. Comparing van der Waals density functionals for CO_2adsorption in metal organic frameworks. *J. Phys. Chem. C* **2012**, *116*, 16957–16968. [CrossRef]
70. Wu, H.; Simmons, J.M.; Srinivas, G.; Zhou, W.; Yildirim, T. Adsorption sites and binding nature of CO_2in prototypical metal−organic frameworks: A combined neutron diffraction and first-principles study. *J. Phys. Chem. Lett.* **2010**, *1*, 1946–1951. [CrossRef]
71. Lim, G.; Lee, K.B.; Ham, H.C. Effect of N-Containing Functional Groups on CO_2 Adsorption of Carbonaceous Materials: A Density Functional Theory Approach. *J. Phys. Chem. C* **2016**, *120*, 8087–8095. [CrossRef]
72. Jahandar Lashaki, M.; Khiavi, S.; Sayari, A. Stability of amine-functionalized CO_2 adsorbents: A multifaceted puzzle. *Chem. Soc. Rev.* **2019**, *48*, 3320–3405. [CrossRef]
73. Ünveren, E.E.; Monkul, B.Ö.; Sarıoğlan, Ş.; Karademir, N.; Alper, E. Solid amine sorbents for CO_2 capture by chemical adsorption: A review. *Petroleum* **2017**, *3*, 37–50. [CrossRef]
74. Young, D.M.; Crowell, A.D. *Physical Adsorption of Gases*; Butterworths: London, UK, 1962.
75. Swaddle, T.W. 6.1.1 Physical Adsorption and Chemisorption. In *Inorganic Chemistry—An Industrial and Environmental Perspective*; Elsevier: Amsterdam, The Netherlands, 1990; pp. 116–117. ISBN 978-0-12-678550-0.
76. Jing, Y.; Wei, L.; Wang, Y.; Yu, Y. Molecular simulation of MCM-41: Structural properties and adsorption of CO_2, N2 and flue gas. *Chem. Eng. J.* **2013**, *220*, 264–275. [CrossRef]
77. Schumacher, C.; Gonzalez, J.; Wright, P.A.; Seaton, N.A. Generation of atomistic models of periodic mesoporous silica by kinetic Monte Carlo simulation of the synthesis of the material. *J. Phys. Chem. B* **2006**, *110*, 319–333. [CrossRef] [PubMed]
78. Sizova, A.A.; Sizov, V.V.; Brodskaya, E.N. Adsorption of CO_2/CH_4 and CO_2/N_2 mixtures in SBA-15 and CMK-5 in the presence of water: A computer simulation study. *Colloids Surf. A Physicochem. Eng. Asp.* **2015**, *474*, 76–84. [CrossRef]
79. Beck, J.S.; Vartuli, J.C.; Roth, W.J.; Leonowicz, M.E.; Kresge, C.T.; Schmitt, K.D.; Chu, C.T.W.; Olson, D.H.; Sheppard, E.W.; McCullen, S.B. A new family of mesoporous molecular sieves prepared with liquid crystal templates. *J. Am. Chem. Soc.* **1992**, *114*, 10834–10843. [CrossRef]
80. Schumacher, K.; Grün, M.; Unger, K.K. Novel synthesis of spherical MCM-48. *Microporous Mesoporous Mater.* **1999**, *27*, 201–206. [CrossRef]
81. Zhao, D.; Sun, J.; Li, Q.; Stucky, G.D. Morphological control of highly ordered mesoporous silica SBA-15. *Chem. Mater.* **2000**, *12*, 275–279. [CrossRef]
82. Neimark, A.V.; Ravikovitch, P.I.; Grün, M.; Schüth, F.; Unger, K.K. Pore size analysis of MCM-41 type adsorbents by means of nitrogen and argon adsorption. *J. Colloid Interface Sci.* **1998**, *207*, 159–169. [CrossRef]
83. Hanwell, M.D.; Curtis, D.E.; Lonie, D.C.; Vandermeersch, T.; Zurek, E.; Hutchison, G.R. Avogadro: An advanced semantic chemical editor, visualization, and analysis platform. *J. Cheminform.* **2012**, *4*, 17. [CrossRef]
84. Humphrey, W.; Dalke, A.; Schulten, K. VMD: Visual Molecular Dynamics. *J. Mol. Graph.* **1996**, *14*, 33–38. [CrossRef] [PubMed]
85. Landmesser, H.; Kosslick, H.; Storek, W.; Fricke, R. Interior surface hydroxyl groups in ordered mesoporous silicates. *Solid State Ion.* **1997**, *101–103*, 271–277. [CrossRef]
86. Van Der Voort, P.; Gillis-D'Hamers, I.; Vrancken, K.C.; Vansant, E.F. Effect of porosity on the distribution and reactivity of hydroxyl groups on the surface of silica gel. *J. Chem. Soc. Faraday Trans.* **1991**, *87*, 3899–3905. [CrossRef]
87. Chang, S.-C.; Chien, S.-Y.; Chen, C.-L. Analyzing adsorption characteristics of CO_2, N_2 and H_2O in MCM-41 silica by molecular simulation. *Appl. Surf. Sci.* **2015**, *331*, 225–233. [CrossRef]
88. Yun, J.-H.; He, Y.; Otero, M.; Düren, T.; Seaton, N.A. Adsorption equilibrium of polar/non-polar mixtures on MCM-41: Experiments and Monte Carlo simulation. In *Studies in Surface Science and Catalysis*; Elsevier: Amsterdam, The Netherlands, 2002; Volume 144, pp. 685–692. ISBN 0167-2991.
89. Yun, J.-H.; Düren, T.; Keil, F.J.; Seaton, N.A. Adsorption of methane, ethane, and their binary mixtures on MCM-41: Experimental evaluation of methods for the prediction of adsorption equilibrium. *Langmuir* **2002**, *18*, 2693–2701. [CrossRef]
90. Arkadi Bezus, B.Y.G.; Kiselev, A.V.; Lopatkin, A.A.; QUANG Du, P.; Bezus, A.G.; Kiselev, A.V.; Lopatkin, A.A.; Du, P.Q. Molecular statistical calculation of the thermodynamic adsorption characteristics of zeolites using the atom–atom approximation. Part 1.—Adsorption of methane by zeolite NaX. *J. Chem. Soc. Faraday Trans. 2 Mol. Chem. Phys.* **1978**, *74*, 367–379.
91. Maddox, M.W.; Olivier, J.P.; Gubbins, K.E. Characterization of MCM-41 using molecular simulation: Heterogeneity effects. *Langmuir* **1997**, *13*, 1737–1745. [CrossRef]
92. Schumacher, C.; Gonzalez, J.; Pérez-Mendoza, M.; Wright, P.A.; Seaton, N.A. Design of Hybrid Organic/Inorganic Adsorbents Based on Periodic Mesoporous Silica. *Ind. Eng. Chem. Res.* **2006**, *45*, 5586–5597. [CrossRef]

93. Williams, C.D.; Travis, K.P.; Burton, N.A.; Harding, J.H. A new method for the generation of realistic atomistic models of siliceous MCM-41. *Microporous Mesoporous Mater.* **2016**, *228*, 215–223. [CrossRef]
94. He, Y.; Seaton, N.A. Experimental and Computer Simulation Studies of the Adsorption of Ethane, Carbon Dioxide, and Their Binary Mixtures in MCM-41. *Langmuir* **2003**, *19*, 10132–10138. [CrossRef]
95. Coasne, B.; Pellenq, R.J.M. Grand canonical Monte Carlo simulation of argon adsorption at the surface of silica nanopores: Effect of pore size, pore morphology, and surface roughness. *J. Chem. Phys.* **2004**, *120*, 2913–2922. [CrossRef] [PubMed]
96. Bhattacharya, S.; Coasne, B.; Hung, F.R.; Gubbins, K.E. Modeling Micelle-Templated Mesoporous Material SBA-15: Atomistic Model and Gas Adsorption Studies. *Langmuir* **2009**, *25*, 5802–5813. [CrossRef]
97. Pellenq, R.J.M.; Levitz, P.E. Capillary condensation in a disordered mesoporous medium: A grand canonical Monte Carlo study. *Mol. Phys.* **2002**, *100*, 2059–2077. [CrossRef]
98. Coasne, B.; Hung, F.R.; Pellenq, R.J.-M.; Siperstein, F.R.; Gubbins, K.E. Adsorption of Simple Gases in MCM-41 Materials: The Role of Surface Roughness. *Langmuir* **2006**, *22*, 194–202. [CrossRef]
99. Couck, S.; Gobechiya, E.; Kirschhock, C.E.A.; Serra-Crespo, P.; Juan-Alcañiz, J.; Martinez Joaristi, A.; Stavitski, E.; Gascon, J.; Kapteijn, F.; Baron, G.V.; et al. Adsorption and Separation of Light Gases on an Amino-Functionalized Metal-Organic Framework: An Adsorption and In Situ XRD Study. *ChemSusChem* **2012**, *5*, 740–750. [CrossRef]
100. Belmabkhout, Y.; Sayari, A. Isothermal versus non-isothermal adsorption-desorption cycling of triamine-grafted pore-expanded MCM-41 mesoporous silica for CO_2 capture from flue gas. *Energy Fuels* **2010**, *24*, 5273–5280. [CrossRef]
101. Pino, L.; Italiano, C.; Vita, A.; Fabiano, C.; Recupero, V. Sorbents with high efficiency for CO_2 capture based on amines-supported carbon for biogas upgrading. *J. Environ. Sci.* **2016**, *48*, 138–150. [CrossRef] [PubMed]
102. Rao, N.; Wang, M.; Shang, Z.; Hou, Y.; Fan, G.; Li, J. CO_2 Adsorption by Amine-Functionalized MCM-41: A Comparison between Impregnation and Grafting Modification Methods. *Energy Fuels* **2018**, *32*, 670–677. [CrossRef]
103. Mafra, L.; Čendak, T.; Schneider, S.; Wiper, P.V.; Pires, J.; Gomes, J.R.B.; Pinto, M.L. Amine functionalized porous silica for CO_2/CH4 separation by adsorption: Which amine and why. *Chem. Eng. J.* **2018**, *336*, 612–621. [CrossRef]
104. Sanz-Pérez, E.S.; Dantas, T.C.M.; Arencibia, A.; Calleja, G.; Guedes, A.P.M.A.; Araujo, A.S.; Sanz, R. Reuse and recycling of amine-functionalized silica materials for CO_2 adsorption. *Chem. Eng. J.* **2017**, *308*, 1021–1033. [CrossRef]
105. Hiyoshi, N.; Yogo, K.; Yashima, T. Adsorption characteristics of carbon dioxide on organically functionalized SBA-15. *Microporous Mesoporous Mater.* **2005**, *84*, 357–365. [CrossRef]
106. Sanz, R.; Calleja, G.; Arencibia, A.; Sanz-Pérez, E.S. CO_2 capture with pore-expanded MCM-41 silica modified with amino groups by double functionalization. *Microporous Mesoporous Mater.* **2015**, *209*, 165–171. [CrossRef]
107. Chang, F.Y.; Chao, K.J.; Cheng, H.H.; Tan, C.S. Adsorption of CO_2 onto amine-grafted mesoporous silicas. *Sep. Purif. Technol.* **2009**, *70*, 87–95. [CrossRef]
108. Mafra, L.; Schneider, S.; Wiper, P.V.; Gomes, R.B.; Pinto, L. Structure of Chemisorbed CO_2Species in Amine-Functionalized Mesoporous Silicas Studied by Solid-State NMR and Computer Modeling. *J. Am. Chem. Soc.* **2017**, *139*, 389–408. [CrossRef]
109. Kwon, S.; Kwon, H.J.; Choi, J., II; Kim, K.C.; Seo, J.G.; Park, J.E.; You, S.J.; Park, E.D.; Jang, S.S.; Lee, H.C. Enhanced selectivity for CO_2adsorption on mesoporous silica with alkali metal halide due to electrostatic field: A molecular simulation approach. *ACS Appl. Mater. Interfaces* **2017**, *9*, 31683–31690. [CrossRef]
110. Serna-Guerrero, R.; Da'na, E.; Sayari, A. New insights into the interactions of CO_2 with amine-functionalized silica. *Ind. Eng. Chem. Res.* **2008**, *47*, 9406–9412. [CrossRef]
111. Belmabkhout, Y.; Serna-Guerrero, R.; Sayari, A. Adsorption of CO_2 from dry gases on MCM-41 silica at ambient temperature and high pressure. 1: Pure CO_2 adsorption. *Chem. Eng. Sci.* **2009**, *64*, 3721–3728. [CrossRef]
112. Otowa, T.; Tanibata, R.; Itoh, M. Production and adsorption characteristics of MAXSORB: High-surface-area active carbon. *Gas Sep. Purif.* **1993**, *7*, 241–245. [CrossRef]
113. Lu, C.; Bai, H.; Wu, B.; Su, F.; Hwang, J.F. Comparative study of CO_2 capture by carbon nanotubes, activated carbons, and zeolites. *Energy Fuels* **2008**, *22*, 3050–3056. [CrossRef]
114. Drage, T.C.; Blackman, J.M.; Pevida, C.; Snape, C.E. Evaluation of activated carbon adsorbents for CO_2 capture in gasification. *Energy Fuels* **2009**, *23*, 2790–2796. [CrossRef]
115. Wei, H.; Deng, S.; Hu, B.; Chen, Z.; Wang, B.; Huang, J.; Yu, G. Granular Bamboo-Derived Activated Carbon for High CO_2 Adsorption: The Dominant Role of Narrow Micropores. *ChemSusChem* **2012**, *5*, 2354–2360. [CrossRef]
116. Martín, C.F.; Stöckel, E.; Clowes, R.; Adams, D.J.; Cooper, A.I.; Pis, J.J.; Rubiera, F.; Pevida, C. Hypercrosslinked organic polymer networks as potential adsorbents for pre-combustion CO_2 capture. *J. Mater. Chem.* **2011**, *21*, 5475–5483. [CrossRef]
117. Plaza, M.G.; Pevida, C.; Arias, B.; Fermoso, J.; Casal, M.D.; Martín, C.F.; Rubiera, F.; Pis, J.J. Development of low-cost biomass-based adsorbents for postcombustion CO_2 capture. *Fuel* **2009**, *88*, 2442–2447. [CrossRef]
118. González, A.S.; Plaza, M.G.; Rubiera, F.; Pevida, C. Sustainable biomass-based carbon adsorbents for post-combustion CO_2 capture. *Chem. Eng. J.* **2013**, *230*, 456–465. [CrossRef]
119. Presser, V.; Heon, M.; Gogotsi, Y. Carbide-derived carbons—From porous networks to nanotubes and graphene. *Adv. Funct. Mater.* **2011**, *21*, 810–833. [CrossRef]
120. Gogotsi, Y.; Nikitin, A.; Ye, H.; Zhou, W.; Fischer, J.E.; Yi, B.; Foley, H.C.; Barsoum, M.W. Nanoporous carbide-derived carbon with tunable pore size. *Nat. Mater.* **2003**, *2*, 591–594. [CrossRef] [PubMed]

121. Chandra, V.; Yu, S.U.; Kim, S.H.; Yoon, Y.S.; Kim, D.Y.; Kwon, A.H.; Meyyappan, M.; Kim, K.S. Highly selective CO_2 capture on N-doped carbon produced by chemical activation of polypyrrole functionalized graphene sheets. *Chem. Commun.* **2012**, *48*, 735–737. [CrossRef] [PubMed]
122. Sevilla, M.; Fuertes, A.B. Sustainable porous carbons with a superior performance for CO_2 capture. *Energy Environ. Sci.* **2011**, *4*, 1765–1771. [CrossRef]
123. Pevida, C.; Plaza, M.G.; Arias, B.; Fermoso, J.; Rubiera, F.; Pis, J.J. Surface modification of activated carbons for CO_2 capture. *Appl. Surf. Sci.* **2008**, *254*, 7165–7172. [CrossRef]
124. Mosher, K.; He, J.; Liu, Y.; Rupp, E.; Wilcox, J. Molecular simulation of methane adsorption in micro- and mesoporous carbons with applications to coal and gas shale systems. *Int. J. Coal Geol.* **2013**, *109–110*, 36–44. [CrossRef]
125. Cinke, M.; Li, J.; Bauschlicher, C.W.; Ricca, A.; Meyyappan, M. CO_2 adsorption in single-walled carbon nanotubes. *Chem. Phys. Lett.* **2003**, *376*, 761–766. [CrossRef]
126. Kurniawan, Y.; Bhatia, S.K.; Rudolph, V. Simulation of binary mixture adsorption of methane and CO_2 at supercritical conditions in carbons. *AIChE J.* **2006**, *52*, 957–967. [CrossRef]
127. Davies, G.M.; Seaton, N.A. The effect of the choice of pore model on the characterization of the internal structure of microporous carbons using pore size distributions. *Carbon N. Y.* **1998**, *36*, 1473–1490. [CrossRef]
128. Heuchel, M.; Davies, G.M.; Buss, E.; Seaton, N.A. Adsorption of carbon dioxide and methane and their mixtures on an activated carbon: Simulation and experiment. *Langmuir* **1999**, *15*, 8695–8705. [CrossRef]
129. Farmahini, A.H.; Opletal, G.; Bhatia, S.K. Structural modelling of silicon carbide-derived nanoporous carbon by hybrid reverse Monte Carlo simulation. *J. Phys. Chem. C* **2013**, *117*, 14081–14094. [CrossRef]
130. Lu, L.; Nicholson, D.; Bhatia, S.K. Adsorption of CH4 and CH_4/CO_2 mixtures in carbon nanotubes and disordered carbons: A molecular simulation study. *Chem. Eng. Sci.* **2015**, *121*, 268–278. [CrossRef]
131. Zhao, J.; Buldum, A.; Han, J.; Lu, J.P. Gas molecule adsorption in carbon nanotubes and nanotube bundles. *Nanotechnology* **2002**, *13*, 195–200. [CrossRef]
132. Xiao, J.; Sitamraju, S.; Janik, M.J. CO_2 adsorption thermodynamics over N-substituted/grafted graphanes: A DFT study. *Langmuir* **2014**, *30*, 1837–1844. [CrossRef] [PubMed]
133. Knowles, G.P.; Graham, J.V.; Delaney, S.W.; Chaffee, A.L. Aminopropyl-functionalized mesoporous silicas as CO_2 adsorbents. *Fuel Process. Technol.* **2005**, *86*, 1435–1448. [CrossRef]
134. Philemon, K.T.; Korir, K.K. Carbon dioxide gas sensing, capture, and storage potential of calcium oxide surface and single walled carbon nanotube: Insights from ab initio simulation. *J. Phys. Condens. Matter* **2020**, *32*, 245901. [CrossRef]
135. Tan, L.; Tan, B. Hypercrosslinked porous polymer materials: Design, synthesis, and applications. *Chem. Soc. Rev.* **2017**, *46*, 3322–3356. [CrossRef] [PubMed]
136. Lu, W.; Yuan, D.; Sculley, J.; Zhao, D.; Krishna, R.; Zhou, H.C. Sulfonate-grafted porous polymer networks for preferential CO_2 adsorption at low pressure. *J. Am. Chem. Soc.* **2011**, *133*, 18126–18129. [CrossRef]
137. James, A.; Reynolds, J.; Reed, D.; Styring, P.; Dawson, R. A Pressure Swing Approach to Selective CO_2 Sequestration Using Functionalised Hypercrosslinked Polymers. *ChemRxiv* **2019**, preprint. [CrossRef]
138. Sun, L.B.; Kang, Y.H.; Shi, Y.Q.; Jiang, Y.; Liu, X.Q. Highly Selective Capture of the Greenhouse Gas CO_2 in Polymers. *ACS Sustain. Chem. Eng.* **2015**, *3*, 3077–3085. [CrossRef]
139. Xu, C.; Hedin, N. Microporous adsorbents for CO_2 capture—A case for microporous polymers? *Mater. Today* **2014**, *17*, 397–403. [CrossRef]
140. Fang, W.; Zhang, L.; Jiang, J. Polymers of intrinsic microporosity for gas permeation: A molecular simulation study. *Mol. Simul.* **2010**, *36*, 992–1003. [CrossRef]
141. Sun, Y.; Wang, L.; Wang, R.; Zheng, S.; Liao, X.; Zhu, Z.; Zhao, Y. Insight on microscopic mechanisms of CH_4 and CO_2 adsorption of coal with different ranks. *Fuel* **2022**, *330*, 125715. [CrossRef]
142. Hasegawa, Y.; Abe, C. Prediction of Adsorption and Diffusion Behaviors of CO_2 and CH_4 in All-Silica Zeolites Using Molecular Simulation. *Membranes* **2021**, *11*, 392. [CrossRef] [PubMed]
143. Tang, D.; Kupgan, G.; Colina, C.M.; Sholl, D.S. Rapid Prediction of Adsorption Isotherms of a Diverse Range of Molecules in Hyper-Cross-Linked Polymers. *J. Phys. Chem. C* **2019**, *123*, 17884–17893. [CrossRef]
144. Yilmaz, G.; Ozcan, A.; Keskin, S. Computational screening of ZIFs for CO_2 separations. *Mol. Simul.* **2014**, *41*, 713–726. [CrossRef]
145. Khosrowshahi, M.S.; Abdol, M.A.; Mashhadimoslem, H.; Khakpour, E.; Emrooz, H.B.M.; Sadeghzadeh, S.; Ghaemi, A. The role of surface chemistry on CO_2 adsorption in biomass-derived porous carbons by experimental results and molecular dynamics simulations. *Sci. Rep.* **2022**, *12*, 8917. [CrossRef]
146. Gomaa, I.; Guerrero, J.; Heidari, Z.; Espinoza, D.N. Experimental Measurements and Molecular Simulation of Carbon Dioxide Adsorption on Carbon Surface. In *SPE Annual Technical Conference and Exhibition*; OnePetro: Richardson, TX, USA, 2022. [CrossRef]
147. Ma, X.; Xu, W.; Su, R.; Shao, L.; Zeng, Z.; Li, L.; Wang, H. Insights into CO_2 capture in porous carbons from machine learning, experiments and molecular simulation. *Sep. Purif. Technol.* **2023**, *306*, 122521. [CrossRef]

Disclaimer/Publisher's Note: The statements, opinions and data contained in all publications are solely those of the individual author(s) and contributor(s) and not of MDPI and/or the editor(s). MDPI and/or the editor(s) disclaim responsibility for any injury to people or property resulting from any ideas, methods, instructions or products referred to in the content.



https://dspace.org/

Molecular simulation techniques as applied to silica and carbon-based adsorbents for carbon capture

Wadi, Basil; Golmakani, Ayub; Borhani, Tohid N.; Manovic, Vasilije; Nabavi, Seyed Ali

2023-07-01
MDPI
https://doi.org/10.3390/en16135013
Wadi B, Golmakani A, Borhani TN, et al., (2023) Molecular simulation techniques as applied to silica and carbon-based adsorbents for carbon capture. Energies, Volume 16, Issue 13, July 2023, Article Number 5013

Downloaded from a DSpace repository. https://dspace.org/